SAND2018-13355C

Φ-Sensitivity for LTGC Engines: Understanding the Fundamentals and Tailoring Fuel Blends to Maximize this Property

Author, co-author (Do NOT enter this information. It will be pulled from participant tab in MyTechZone)

Affiliation (Do NOT enter this information. It will be pulled from participant tab in MyTechZone)

Abstract

φ-sensitivity is a fuel property that has important benefits for the operation and control of LTGC engines. A fuel is φ-sensitive if its autoignition reactivity varies with the fuel/air equivalence ratio (φ). Thus, multiple-injection strategies can be used to create a φ-distribution that leads to several benefits. First, the φ-distribution causes a sequential autoignition that reduces the HRR peak. This allows higher loads without knock and/or CA50 to be advanced for higher efficiencies. Second, CA50 can be controlled by the late-DI settings of a multiple-injection strategy. Finally, experiments show that ITHR (intermediate-temperature heat release) increases with φ-sensitivity, increasing the allowable CA50 retard and stability.

CHEMKIN simulations were performed using a detailed mechanism to understand the chemistry responsible for φ-sensitivity. For fuels with NTC behavior, φ-sensitivity is greatest in the NTC region due to enhanced ITHR reactions, which explains the experimental correlation between φ-sensitivity and ITHR. Under engine conditions, higher intake pressure means lower intake temperature to balance the reactivity, and both effects increase the φ-sensitivity. However, φ-sensitivity remains almost constant if decreased oxygen concentration is used to control the reactivity increase with intake-pressure boost because pressure and oxygen have opposite effects. Finally, for fuels without an NTC regime, φ-sensitivity is lower and almost constant as operating conditions vary.

The potential of designing fuel blends that increase the φ-sensitivity compared to RD5-87 (regular E10 gasoline), while maintaining high RON and octane-sensitivity, was investigated. Higher φ-sensitivity and higher RON than RD5-87 can be reached with a 5-component blend that fulfill U.S. regulations. The fuel mixture is composed by a combination of olefins (1-hexene), paraffins (n-pentane and iso-octane), aromatics (p-xylene) and alcohols (iso-butanol, which was recently approved by the E.P.A. for gasoline blending). This study shows that it should be possible to have both high φ-sensitivity and high RON with good octane-sensitivity.

Introduction

Starting with the interest in Homogeneous Charge Compression Ignition (HCCI) in the latter 1990s, many Low Temperature Combustion (LTC) strategies have been studied in recent years because they offer high efficiencies (≥ diesel-engine efficiencies) with very low NO_x and soot emissions [1 – 3]. Unlike diesel combustion, LTC avoids combustion at rich equivalence ratios and high temperatures where soot and NO_x form, respectively, as illustrated in Kamimoto's equivalence ratio versus temperature diagram [1, 4]. However, it is also important to keep LTC combustion temperatures above about 1500 K to obtain good combustion efficiency and to minimize CO emissions [1, 2], and unburned hydrocarbon (HC) emissions, which can arise from near-wall and crevice regions [5].

With the need to reduce fuel consumption and CO_2 emissions, LTC is of particular interest an alternative to conventional spark-ignition (SI) gasoline combustion because it offers substantially higher thermal efficiencies. There are four main reasons why Low Temperature Gasoline Combustion (LTGC) engines show higher efficiencies than SI engines. First, the lean equivalence ratios and low combustion temperatures of LTGC engines result in a significantly higher specific heat ratio (c_p/c_v) than for spark-ignition (SI) engines, increasing the efficiency. Second, heat losses are reduced due to the lower combustion temperatures. Third, LTGC engines typically have higher compression ratios than standard SI engines. Finally, pumping work is also lower in LTGC engines because they are typically not throttled. However, several technical challenges must be overcome prior to the implementation of LTGC in commercial engines, with two of the most important being extending LTGC operation to higher loads and improving combustion-timing control.

Historically, well-mixed LTGC operation (i.e. HCCI) has been limited to low-to-medium engine loads because increasing the fueling rate at a given intake pressure increases the maximum cylinder-pressure rise rate (PRR_{max}), eventually causing engine knock or even engine damage. Retarding the combustion timing can reduce these high PRR_{max} values, but the amount of timing retard is limited by poor combustion stability and eventually misfire [5, 6]. As the fueling is increased, the range of crank angle degrees (CAD) available to control the combustion phasing without knock or misfire becomes narrower. Thus, there is a condition at which stable autoignition can be reached but no control on the combustion phasing is available, since slightly more fueling will lead to knock and slightly more retarded combustion will lead to misfire. This condition is called the knock/stability limit, and it defines the maximum engine load that can be reached at a given set of engine conditions.

In a real engine, naturally occurring thermal stratification develops due to wall heat transfer and turbulent convection [7 – 10], which causes the charge to autoignite sequentially from the hottest regions to the coldest [7, 11]. This sequential autoignition extends the burn duration and significantly reduces the peak heat release rate (HRR), extending the load limit significantly compared to a thermally homogeneous charge. Moreover, retard the timing has been shown to amplify the effect of the stratification, further extending the load limit [7, 11]. In fact, Kodavasal et al. [12] showed that thermal stratification dominates the ignition under well-mixed HCCI operation. It should be noted that because thermal stratification occurs naturally in all real engines, its benefits for reducing the HRR and are included when determining the knock/stability limit experimentally. In theory, it should be possible to significantly extend the load limit by increasing the thermal stratification [11], but achieving this using practical methods and without increasing heat losses has proven difficult [1, 6, 13].

Another method that has been demonstrated to extend the knock/stability limit for higher loads is to increase the stability by using fuels or operating conditions that result in a greater amount of Intermediate Temperature Heat Release (ITHR). ITHR results from the early reactions that ramp the combustion up into hot autoignition [7, 14, 15], and as the name indicates, it occurs at temperatures below the hot-ignition temperature and above those of the low-temperature heat release (LTHR) if the latter is present. The ITHR keeps the bulk-gas temperatures rising during the early expansion stroke, providing combustion stability as timing is retarded. Increasing the ITHR allows greater combustion-timing retard with good stability, which shifts the knock/stability limit to later crank angles allowing higher loads. The importance of this effect on combustion stability and timing retard limits was first reported for PRF80 at naturally aspirated conditions [16]. Because PRF80 showed two-stage ignition, it was initially thought that LTHR was required to gain this benefit. However, Dec and Yang [17] later showed that for a regular-grade (AKI=87) gasoline, the ITHR increased substantially as intake boost pressure was increased even though little or no LTHR was observed. The increased ITHR allowed them greatly increase the combustion-timing retard to prevent knock for high fueling rates at high boost pressures. As a result, they were able to obtain a gross Indicated Mean Effective Pressures (IMEPg) above 16 bar for well-mixed LTGC (i.e. HCCI). However, this required an intake pressure of 3.2 bar absolute, which may be unrealistically high for a turbocharger with this engine load.

Perhaps the most promising strategy to extend LTGC engine loads is to use fuel stratification to produce a sequential autoignition event. Unlike thermal stratification which is difficult to enhance and control, fuel stratification can be readily controlled by varying the Direct-Injection (DI) fueling strategy. For fuel stratification to be effective for controlling the heat release rate, the different local equivalence ratios within the stratified mixture must have different ignition delays [18] to produce the required sequential autoignition. This capability of the fuel is termed its φ-sensitivity, and φ-sensitivities have been directly measured for several fuels [18 – 20]. Initially, φ-sensitivities were measured only at naturally aspirated conditions for a limited number of fuels, and it was thought that two-stage ignition was required for fuels to be φ-sensitive [18, 19]. However, later studies showed that two-stage ignition (i.e. LTHR) was not required and that φ-sensitivity was actually correlated with the ITHR. The ITHR is typically higher for two-stage fuels, but similar ITHRs can occur with single-stage ignition fuels under boosted conditions, as will be discussed further below.

Early attempts at fuel stratification simply tried various DI-fueling strategies in HCCI engines without knowledge of the importance of fuel effects and φ-sensitivity. Marriott and Reitz [21] investigated the capability of controlling the combustion phasing by fuel stratification in an engine fueled with iso-octane at P_{in} = 1.0 bar. They concluded that the combustion process could be properly phased by means of fuel stratification only at low engine loads, since stratification led to faster heat release rates and, therefore, the stratified operating range was easily knock limited. This was most likely the result of iso-octane's negligible φ-sensitivity at the P_{in} = 1.0 bar conditions tested. Later, Kalghatgi et al. [22] tried to extend the engine load of a single-cylinder DI diesel-type Compression Ignition (CI) engine fueled with conventional gasoline by applying different injection strategies with the intent of promoting fuel stratification. They obtained IMEP values up to 15.95 bar; however, the fuel stratification needed to reach such load led to NO_x emissions that were much higher than the US 2010 limit. This issue could potentially be resolved with more carefully controlled fuel stratification and ensuring that the fuel was φ-sensitive under the conditions studied. In fact, Sjöberg and Dec [18] experimentally evaluated the ability of PRF80 and PRF83 to increase the engine load by stratifying the mixture in a naturally aspirated LTGC engine. These fuels were select because separate tests showed that they were φ-sensitive at this operating condition. Moreover, they [18] developed a specialized fuel stratification technique, based on multi-zone kinetic modeling, called partial fuel stratification (PFS), in which the majority of the charge (~80-90%) was injected early in the intake stroke (or premixed) while remainder was injected during the latter half of the compression stroke. The timing and fuel-fraction of this second-DI fueling were varied to control the amount of stratification. With this approach, they obtained higher maximum IMEPg values, compared to a well-premixed charge, without knock or misfire, and while keeping NO_x emissions at acceptable levels. These findings are supported by Yang et al. [14, 15, 23] who showed that PFS with φ-sensitive fuels could significantly reduce the PRR_{max} compared to premixed fueling for both PRF73 and a low-octane gasoline. Furthermore, in [15] they showed that because PFS reduced the PRR_{max} at a given engine condition, combustion phasing (i.e. the 50% burn point or CA50) could then be advanced to obtain higher thermal efficiency without exceeding the same PRR_{max} as the original premixed operation. These findings are also consistent with the works of Wada and Senda [24] and Dahl et al. [25] who studied the effects of fuel stratification using two-stage ignition fuels that were φ-sensitive under the naturally aspirated conditions of their tests.

These early demonstrations of the benefits of applying fuel stratification were conducted using two-stage ignition fuels that show φ-sensitivity at naturally aspirated (P_{in} = 1.0 bar) conditions. Subsequently, Dec et al. [20] showed that regular-grade (87 AKI) gasoline which is not φ-sensitive at P_{in} = 1.0 bar conditions becomes progressively more φ-sensitive as the intake pressure is increased from 1.0 to 2.0 bar. In fact, it is more φ-sensitive at P_{in} = 2.0 bar than PRF 73 (a two-stage fuel) is at P_{in} = 1.0 bar, even though it shows virtually no LTHR at these boosted conditions, only enhanced ITHR. Dec et al. [20] then applied PFS using this gasoline, showing that it could reduce the HRR at $2.2 \leq P_{in} \leq 2.4$ bar, which allowed them to obtain higher loads without engine knock and with good stability, and/or to advance CA50 for higher efficiencies. These changes in φ-sensitivity with intake boost correspond extremely well with the amount of ITHR enhancement with boost, which also allows greater timing retard with good stability [17], as discussed above. Subsequent to this work, Yang et al. [15] examined ITHRs and φ-sensitivities of both a low-octane gasoline that exhibited two-stage ignition and this regular-grade gasoline under boosted conditions which showed only single-stage ignition (using the data from Refs. [17, 20]), and they linked the φ-sensitivity to the intensity of the ITHR for both fuels. These authors found that the more intense the ITHR, the higher the φ-sensitivity. An initial attempt to understand the chemical kinetics behind the ITHR were performed by Mehl et al. [26]. They concluded that the chemical nature of the ITHR is significantly different from the chemical nature of the Low Temperature Heat Release (LTHR). However, these authors did not explore the relationship between the magnitude of the ITHR and the φ-sensitivity. Other more recent experimental studies of fuel stratification to extend the engine load for HCCI/LTGC combustion include, Lee et al. [27], Li et al. [28] and Shen et al. [29].; however, φ-sensitivity fundamentals were not studied in these investigations either.

In addition to reducing the HRR to allow higher loads without knock or more advanced CA50 for higher efficiencies, varying the amount of fuel stratification under φ-sensitive conditions can be used for combustion-phasing control. The potential of this effect was shown by Dec and Sjöberg [19] who contrasted the changes in CA50 as injection timing was varied for both a φ-sensitive and a non-φ-sensitive fuel. In a more recent work, Gentz et al. [30] showed that PFS with a variable second-DI timing to adjust the amount of stratification could control CA50 from advanced timings that gave strong knock to retarded timings near the misfire limit. Because CA50 is controlled by the DI fuel-injection, CA50 can be adjusted from one cycle to the next. This control techniques was successfully applied over a range of intake pressures from 1.0 to 2.4 bar using a regular-grade (87 AKI) E10 gasoline. However, performance of this technique at naturally aspirated and low-boost conditions was not as good as at higher intake pressures, indicating that it would be advantageous to have a fuel with increased φ-sensitivity at lower intake pressures. Although they did not relate this behavior to φ-sensitivity, several authors have used fuel stratification strategies with the intent of controlling CA50, such as Kalghatgi et al. [22], Johansson et al. [31], and Sellnau et al. [32].

Despite the fact that the literature contains numerous studies in which the φ-sensitivity is used to both extend the engine load and control the combustion phasing, very little is known about the chemical kinetics that control this property. Moreover, most investigations did not even explore the relationship between the effects of fuel stratification and the φ-sensitivity. A better understanding of the causes of φ-sensitivity and its relationship to the ITHR is needed to develop fuels that enhance this behavior at the operating conditions of interest, so that the advantages of φ-sensitivity can be exploited for improved LTGC-engine performance as described above.

Finally, although increasing the φ-sensitivity has advantages for controlling the maximum PRR and CA50, it is also important not to enhance this property at the expense of giving the fuel poor autoignition resistance at high-load conditions. The autoignition reactivity of the fuel has to be sufficiently limited to allow LTGC operation at high boost conditions needed for high loads and/or to allow SI combustion to achieve high engine loads for mixed-mode operating strategies. Therefore, high φ-sensitivity fuels need to also have high Research Octane Number (RON) and octane-sensitivity values.

Two research gaps can be identified from the literature review discussed in the previous paragraphs. On the one hand, little is known about the chemical kinetics that cause the φ-sensitivity. On the other hand, a fuel that enhances this property while showing high autoignition resistance is needed. Thus, the two main objectives of the current study are:

1) To identify the chemical kinetics responsible for the φ-sensitivity and to explain the relationship between φ-sensitivity and ITHR. To accomplish this, the φ-sensitivities of 8 single-component fuels are analyzed by means of chemical kinetic simulations carried out in CHEMKIN with a detailed chemical kinetic mechanism.
2) To explore the potential of developing a fuel that has both high φ-sensitivity and low reactivity at high engine-load conditions (i.e. high RON and high octane-sensitivity), compared to the values for a regular-grade E10 gasoline. This is accomplished by combining representative species of several of the main hydrocarbon classes to obtain multi-component blends that maximize the φ-sensitivity while keeping the RON and octane sensitivity in acceptable ranges. The U.S. regulations limiting the amount of some hydrocarbon classes in gasoline (e.g. aromatics) are also considered when developing these new fuel blends.

Following this introduction, a description of the general methodology applied in this investigation is presented. Then, the results of the study are presented in two parts corresponding to the two objectives listed above. In the final section, the work is summarized and conclusions are drawn.

General Methodology

ANSYS CHEMKIN-PRO 18.1 is the software used to perform the chemical simulations. An unpublished detailed chemical kinetic mechanism for gasoline surrogates from Lawrence Livermore National Laboratory (LLNL) is used these simulations to obtain the ignition characteristics of all fuels tested in this investigation. The mechanism consists of 2027 species and 8619 reactions, including 215 reactions to describe NO_x chemistry. It is an updated version of the free-access chemical kinetic mechanism available in LLNL's website [33], which has been widely validated versus experimental data [34].

Sandia's LTGC/HCCI research engine is used to exemplify engine-like conditions in this investigation. Engine results are obtained by imposing the geometric characteristics of Sandia's engine [15], which are given in Table 1, on a 0-D, adiabatic, closed, internal combustion engine reactor (IC-engine) in CHEMKIN. The experimental facility has the ability of providing a fully premixed charge to the engine by vaporizing the fuel in an electrically heated chamber and mixing it with the air well upstream of the intake plenum. However, a minimum intake temperature of 333 K is required to avoid fuel condensation in the intake system. It has been experimentally determined that a 333 K intake temperature results in a temperature at Bottom Dead Center (BDC) of ≈360 K due to heat transfer through the walls of the intake port and combustion chamber (which are held to 100°C by heating the "cooling" water) and mixing with the hot residuals. This technical limitation is also imposed on the engine model. Thus, the minimum temperature at BDC, which corresponds to the minimum initial temperature in the simulations, is equal to 360 K.

Table 1. Characteristics of Sandia's LTGC/HCCI research engine.

Displacement (single cylinder)	0.981	dm^3
Bore	102	mm
Stroke	120	mm
Connecting Rod Length	192	mm
Geometric Compression Ratio	14:1	-
Effective Compression Ratio	13.3:1	-

An equivalence ratio based on the total charge mass is used in engine simulations, which definition is the following:

$$\boldsymbol{\varphi}_{\mathbf{m}} = \frac{\mathbf{F/C}}{\mathbf{F/A_{st}}} \quad \mathbf{(1)}$$

Where *F/C* is the mass ratio between fuel and air + EGR, and F/A_{st} is the fuel-air mass ratio under stoichiometric conditions. This equivalence ratio definition allows comparing data with the same supplied energy content per unit charge mass for either lean or EGR-diluted conditions. It should be noted that φ_m is the same as the conventional air-based φ when no EGR is used.

Top Dead Center (TDC) intake is defined as 0 CAD, thus, TDC compression is equal to 360 CAD. This criterion avoids using negative values for the crank angle or a nomenclature that distinguishes between before and after TDC. The crank angle of the 50% burn point (CA50) is used as indicator of the combustion phasing. Finally, all engine conditions have an engine speed equal to 1200 rpm.

In order to estimate the effect of stratifying the charge on the local temperature, the relative variation in temperature caused by a variation in equivalence ratio is estimated by taking into account the heat of vaporization of the fuel (*HoV*) as follows:

$$\Delta\boldsymbol{\varphi}\ \boldsymbol{HoV}\frac{\boldsymbol{F}}{\boldsymbol{A_{st}}} = \left(\boldsymbol{\varphi}\frac{\boldsymbol{F}}{\boldsymbol{A_{st}}} + \mathbf{1}\right)\boldsymbol{C_p}\Delta\boldsymbol{T} \quad \mathbf{(2)}$$

where C_p is the heat capacity of the air/fuel mixture at the temperature of interest. Thus, starting from a certain temperature condition, Eq. 2 can be used to estimate temperature variations ($\Delta\boldsymbol{T}$) caused by equivalence ratio variations ($\Delta\boldsymbol{\varphi}$) when a fuel distribution is generated, for instance, by a direct injection event. It should be noted that the effect of the specific heat ratio distribution during the ignition delay, as well as the effects of heat losses, convection and turbulence, are not taken into account. Therefore, thermal stratification is expected to be higher in a real engine.

Φ-Sensitivity Fundamentals

Methodology: Sensitivity analyses in constant-volume reactors

For the sensitivity analyses, a 0-D, adiabatic, closed reactor is modeled in CHEMKIN, in which constant volume conditions are imposed and the pressure and temperature evolutions are obtained by solving the energy equation and the equation of state.

Three different ignition stages are defined in this work, the ignition delays of which correspond to the end of each stage:

1. Low Temperature Heat Release (LTHR): From the start of the simulation up to the instant at which the HRR signal reaches a relative minimum located between HRR peaks. It is only defined if a two-stage ignition pattern occurs.
2. Intermediate Temperature Heat Release (ITHR): From the end of the LTHR up to the instant at which the maximum H_2O_2 consumption rate occurs. H_2O_2 decomposition is chosen as ignition tracer because it triggers the high-temperature ignition stage. ITHR is defined from the start of the simulation in case of having a single-stage ignition pattern (no LTHR).
3. High Temperature Heat Release (HTHR): From the end of the ITHR up to the end of the simulation.

Figure 1 shows the definition of the three different ignition stages considered in this investigation. Both the HRR signal, which is plotted in logarithmic scale, and the H_2O_2 decomposition signal are included in the figure. The ignition delay referred to the end of the ITHR stage (τ) is used to calculate the φ-sensitivity, which is defined as follows:

$$\varphi - \text{sensitivity} = \frac{d\tau}{d\varphi} \quad (3)$$

It should be noted that richer mixtures lead to faster ignition if the other conditions remain constant (i.e., the higher the equivalence ratio, the shorter the ignition delay). Thus, the φ-sensitivity defined by Eq. 3 will have negative values when the pressure, temperature and oxygen content are constant.

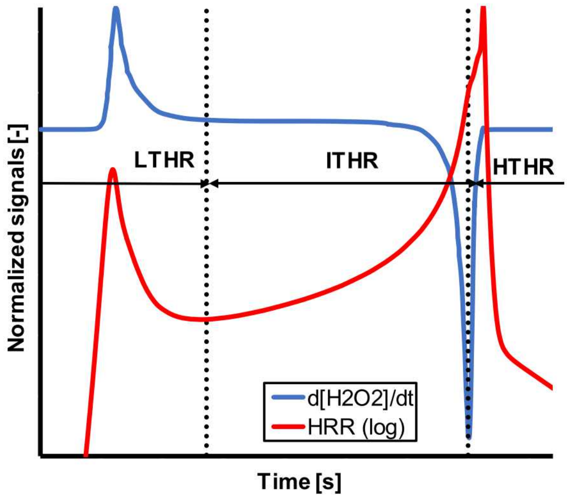

Figure 1. Typical HRR (in logarithmic scale) and H_2O_2 decomposition. The three different ignition stages considered in this investigation are defined in the figure.

Sensitivity analyses are carried out to identify the chemical reactions that have a greater effect on the change in ignition delay when the equivalence ratio is varied, i.e., on the φ-sensitivity. To do so, the following sensitivity coefficients have been calculated at the time of ignition:

$$S_i = \frac{\partial}{\partial\varphi}\left(\frac{A_i}{T_{max} - T_0}\frac{\partial T}{\partial A_i}\right) \quad (4)$$

S_i, which is a dimensionless coefficient, measures how much the φ-sensitivity is affected by reaction *i*. A_i represents the pre-exponential factor of reaction *i*. The term inside the brackets is the temperature A-factor sensitivity and it is calculated by CHEMKIN. It should be noted that temperature sensitivity at the time of ignition is equivalent to ignition delay sensitivity, since the temperature rise is uniquely caused by the ignition event. S_i is normalized by the temperature rise caused by the combustion, which is proportional to the amount of heat released. This way, simulations with different equivalence ratios can be properly compared. Additionally, the contribution of each reaction to the heat released during each ignition stage is calculated. Thus, the reactions responsible for the LTHR, ITHR and HTHR can be identified.

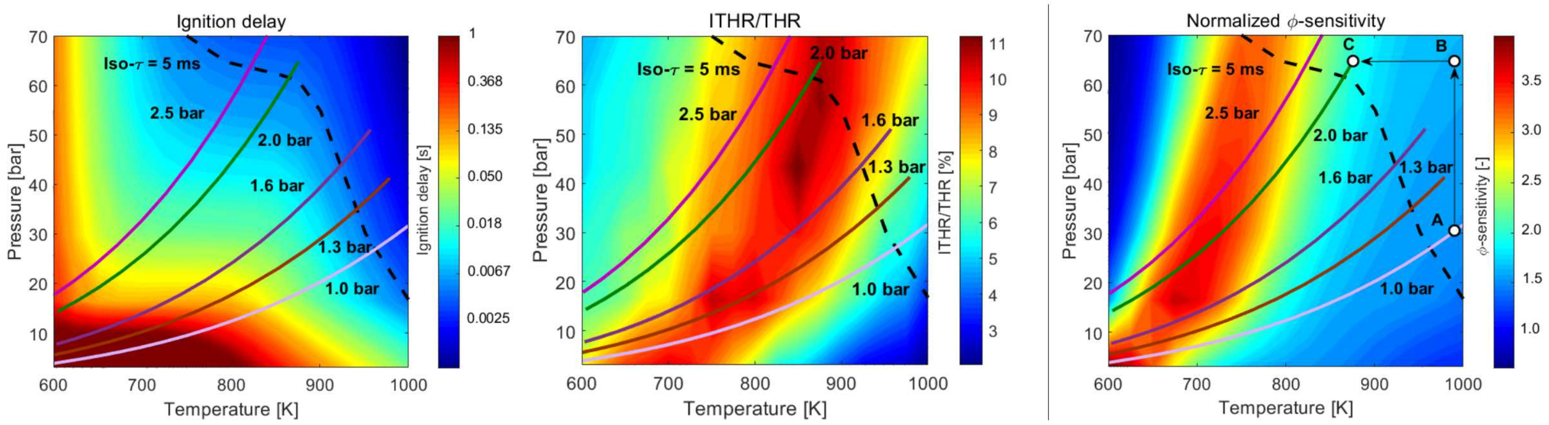

Figure 2. Ignition delay map (left), ITHR intensity map (center) and normalized φ-sensitivity map (right) for iso-octane at $\varphi_m = 0.40$ and $X_{O2} = 21\%$. The iso-ignition delay curve that corresponds to 5 ms, which is considered the threshold between useful and useless operating conditions, is plotted in dashed line. Finally, the in-cylinder temperature vs pressure evolutions for iso-octane at Pin = 1.0, 1.3, 1.6, 2.0 and 2.5 bar and constant CA50 = 368.5 CAD are also plotted in the figure.

Table 2 shows the single-component fuels tested in this study, which are denoted with the name used in the chemical kinetic mechanism. The tested fuels represent the hydrocarbon classes usually presented in commercial gasolines. Furthermore, RON values from 121 (toluene) to 0 (n-heptane) were included in this study.

The following operating conditions are tested:

- Pressure (P): from 3 bar to 70 bar in steps of 13.4 bar.
- Temperature (T): from 600 K to 1000 K in steps of 25 K.
- Equivalence ratio (φ): from 0.30 to 0.80 in steps of 0.05.
- Oxygen molar fraction (X_{O2}): from 0.21 to 0.105 in steps of 0.01.

It should be noted that almost all the operating range of HCCI engines is covered by this test matrix.

Table 2. Single-component fuels tested in this investigation.

Hydrocarbon class	Species	Name
Paraffins	N-pentane	NC5H12
	N-heptane	NC7H16
Iso-paraffins	Iso-octane	IC8
Cyclo-paraffins	Cyclo-pentane	CPT
Aromatics	Toluene	C6H5CH3
Olefins	Di-iso-butylene	IC8D4
	1-Hexene	C6H12-1
Oxygenated	Ethanol	C2H5OH

Results and Discussion: Φ-Sensitivity Fundamentals

The chemical kinetics responsible for φ-sensitivity are analyzed in this section. To do so, fuels shown in Table 2 are separately studied depending on whether or not they show NTC behavior. It should be noted that fuels that show NTC behavior can ignite in three different temperature regimes, and different chemical paths control the reactivity in each regime. Therefore, the chemical reactions responsible for the φ-sensitivity are expected to be different depending on the operating conditions.

Fuels that show NTC behavior

Figure 2 shows the ignition delay (in logarithmic scale), ITHR intensity and normalized φ-sensitivity for iso-octane at $\varphi_m = 0.40$ and $X_{O2} = 21\%$. Iso-octane is the fuel shown in all the figures of this sub-section because it has both NTC behavior and similar reactivity to a conventional gasoline. However, analogous results can be obtained with other fuels that also show NTC behavior.

The ignition delay, ITHR intensity and normalized φ-sensitivity are plotted in pressure-vs-temperature maps in order to analyze the behavior of these properties at different temperature regimes. First, the ITHR intensity is defined as the contribution of the ITHR to the total amount of heat, in percent (i.e., ITHR intensity is equal to the heat released during the ITHR divided by the total heat released). Second, the φ-sensitivity should be normalized in order to properly compare conditions that have very different ignition delays. The normalization of the φ-sensitivity is performed as follows:

$$\text{Norm}(\varphi - \text{sensitivity}) = -\frac{1}{\tau}\frac{d\tau}{d\varphi} \quad (5)$$

The normalized φ-sensitivity has the opposite sign of the φ-sensitivity defined by Eq. 3 in order to avoid negative values, improving the readability of the plots. The reader should remember that higher equivalence ratios lead to shorter ignition delays and, therefore, $d\tau/d\varphi$ is negative. The normalized φ-sensitivity at a certain equivalence ratio is numerically calculated using Newton's difference quotient with a step value equal to +0.05.

Figure 2 also shows the iso-ignition delay curve that corresponds to 5 ms (black dashed line) as an indicator of the working range for iso-octane in LTGC engines (the use of a threshold equal to 5 ms is justified in Appendix B). Thus, operating conditions below the dashed line are not useful for LTGC engines fueled with iso-octane because they have too long ignition timescales. The reader should notice that analogous results as the ones shown for iso-octane can be seen with other fuels that also show NTC behavior. However, the NTC zone, the iso-ignition delay line that limits the useful conditions for LTGC engines, the ITHR intensity and the φ-sensitivity will shift if a different fuel is tested. Therefore, the trends shown by Fig. 2 will be seen also for other NTC fuels but with a different location in the pressure-vs-temperature maps.

NTC and pressure effects on φ-sensitivity

Also shown in Fig. 2 are five pressure-vs-temperature trajectories that correspond to P_{in} = 1.0, 1.3, 1.6, 2.0 and 2.5 bar. These trajectories are obtained by solving an IC-engine reactor fueled with iso-octane in which CA50 = 368.5 CAD. The combustion phasing is controlled by adjusting the BDC temperature and, once the minimum value allowable in Sandia's engine is reached (360 K), by adding EGR. As it can be seen for naturally aspirated conditions, LTGC engines use to work at high temperature and the hot-side of the NTC zone is only reached when high-boosted conditions are tested. The map shows that iso-octane has very low φ-sensitivity values at P_{in} = 1.0 bar, while high φ-sensitivity levels are reached when $P_{in} > 1.6$ bar because ignition occurs closer to the NTC zone. Ignitions slightly dominated by the NTC zone are highly desirable to promote a sequential autoignition controlled by a stratified mixture. These results agree with the experimental measurements performed by Dec and Sjöberg [19], Sjöberg and Dec [18], Dec et al. [20] and Yang et al. [14], concluding that fuels that show a two-stage ignition are more prone to show high φ-sensitivity. As explained before, the position of the NTC zone in the pressure-vs-temperature map will shift for different fuels. Thus, high φ-sensitivity values under naturally aspirated conditions could be obtained with other fuels different from iso-octane. Sjöberg and Dec [18] and Yang et al. [14] explored this idea by comparing the combustion characteristics under stratified conditions of PRF80 and PRF83 [18], and PRF73 [14] versus iso-octane at P_{in} = 1.0 bar. PRF blends showed a two-stage ignition and fuel stratification effectively reduced the maximum pressure rise rate. However, this behavior could not be seen for iso-octane, since this fuel is not φ-sensitive at naturally aspirated conditions. Finally, Fig. 2 shows that the highest φ-sensitivity levels are reached on the cold-side of the NTC zone. In fact, the maximum φ-sensitivity occurs at the cold-side of NTC. It should be noted that the φ-sensitivity has almost negligible values in the low-temperature regime (north-west corner of the plots), where the ignition is completely controlled by the LTHR. Conversely, the φ-sensitivity still shows significant values in the transition between the NTC and the high-temperature regime.

Figure 2, right-hand plot, illustrates the behavior of the φ-sensitivity with pressure. The NTC zone moves to higher temperatures if the pressure is increased. Thus, starting from typical engine operating conditions (point A) and increasing the pressure, the new operating point (point B) is closer to the NTC regime and the φ-sensitivity increases. Furthermore, the temperature must be decreased when the pressure increases in order to control the reactivity of the mixture (point C), increasing the φ-sensitivity even more.

Φ-sensitivity and ITHR

Comparing the ITHR intensity map and the normalized φ-sensitivity map shown by Fig. 2, it can be seen that both properties follow the same trends but there is an offset between the maximum φ-sensitivity (that occurs at the cold-side of NTC) and the maximum ITHR intensity (that occurs at the hot-side of NTC). This offset depends on the width (in terms of temperature interval) of the NTC zone, i.e., it depends on the relevance of the NTC behavior. However, the ITHR intensity can be used as an indicator of the φ-sensitivity under typical engine conditions. Starting from working conditions in the high-temperature regime (which is a typical situation in naturally aspirated LTGC engines), the φ-sensitivity will be improved if the ITHR intensity increases. Therefore, under engine-like conditions, the higher the ITHR intensity the higher the φ-sensitivity. These results agree with the experimental measurements carried out by Yang et al. [15].

EGR / O_2 effects on φ-sensitivity

The pressure-vs-temperature trajectories plotted in Fig. 2 show that the temperature has to be decreased when increasing the intake pressure to control the reactivity of the mixture. For instance, the temperature at TDC varies from 998.2 K at naturally aspirated conditions to 875.8 K at P_{in} = 2.0 bar. As explained in the *General Methodology* section, a minimum intake temperature equal to 333 K is required in Sandia's LTGC engine in order to avoid fuel condensation in the intake system when working under fully premixed conditions. Thus, the temperature cannot be reduced sufficiently when the intake pressure is boosted from 2.0 bar to 2.5 bar and the reactivity has to be controlled by adding EGR, which reduces the oxygen content of the charge and decreases its autoignition reactivity.

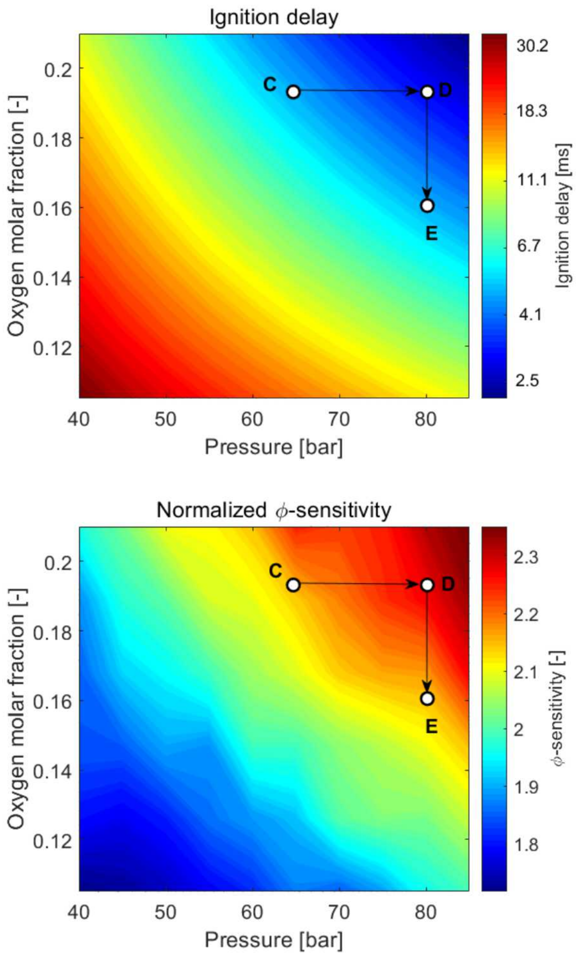

Figure 3. Ignition delay map (top) and normalized φ-sensitivity map (bottom) for iso-octane at φ_m = 0.40 and T = 875.8 K. Point C corresponds to Point C in Fig. 4 - right.

Figure 3 shows the ignition delay (top) and normalized φ-sensitivity (bottom) of iso-octane in an oxygen concentration-vs-pressure map at φ_m = 0.40 and T = 875.8 K, which is the TDC temperature that corresponds to P_{in} = 2.0 bar. Thus, point C in the figure approximately corresponds to point C in Fig. 2 – right. Analogous to increasing the pressure, the NTC moves to higher temperatures if the oxygen concentration increases [35]. Thus, the higher the pressure or the higher the oxygen content, the higher the φ-sensitivity. As expected, the φ-sensitivity increases when the pressure is increased from point C to point D. However, the oxygen content has to be decreased in order to keep the reactivity constant. To do so, the oxygen molar fraction is reduced (i.e., the EGR rate is increased) from point D to point E, which is located on the same iso-ignition delay curve as the starting point C (see Fig. 3 – top). Looking at the φ-sensitivity plot at the bottom of Fig. 3, it can be seen that the φ-sensitivity remains almost constant if decreased oxygen concentration is used to control the reactivity increase with intake-pressure boost because pressure and EGR have opposite effects.

Equivalence ratio effects on φ-sensitivity

Figure 4 shows the effect of the equivalence ratio on the φ-sensitivity by plotting the ignition delay (top) and normalized φ-sensitivity (bottom) of iso-octane in an equivalence ratio-vs-temperature map. The pressure is equal to 64.7 bar, which corresponds to the TDC pressure when $P_{in} \approx 2.0$ bar, and the oxygen concentration is equal to 21% (no EGR). Thus, point C in the figure corresponds to point C in Fig. 2 and 3. An artificial fuel stratification is plotted starting from $\varphi_m = 0.40$ to $\varphi_m = 0.70$ at steps of 0.05. The temperature value that corresponds to each equivalence ratio is calculated by applying Eq. 2, which takes into account the heat of vaporization of the fuel to estimate the relative temperature variation caused by a certain equivalence ratio variation. Fig. 4 – top shows that under typical LTGC engine conditions the richest mixture ignites first. The ignition delay distribution shown in the figure goes from ≈3.9 ms at $\varphi_m = 0.40$ to ≈2.1 ms at $\varphi_m = 0.70$, leading to a sequential autoignition event that takes place during ≈1.8 ms (which corresponds to 13.2 CAD at 1200 rpm). Obviously, the sequential autoignition will be faster in the real engine due to the temperature and pressure rise associated with the first-ignited regions, which compress the remaining charge, and early chemistry occurring during the compression stroke. However, Fig. 4 gives an idea of how the φ-sensitivity leads to a longer, smoother HRR when fuel stratification is applied in the engine.

Figure 4 also shows that, analogously to pressure (Fig. 2) and oxygen content ([35], not shown here), the NTC region is moved to higher temperatures if the equivalence ratio increases. However, richer mixtures show lower φ-sensitivities, i.e., the higher the equivalence ratio the lower the φ-sensitivity. The trends shown by the φ-sensitivity in each temperature regime can be seen in both Fig. 2 – right and Fig. 4 – bottom. The φ-sensitivity is almost negligible during the low-temperature regime (north-west corner of the plots), it reaches a maximum value at the cold-side of NTC and it smoothly decreases during the high-temperature regime.

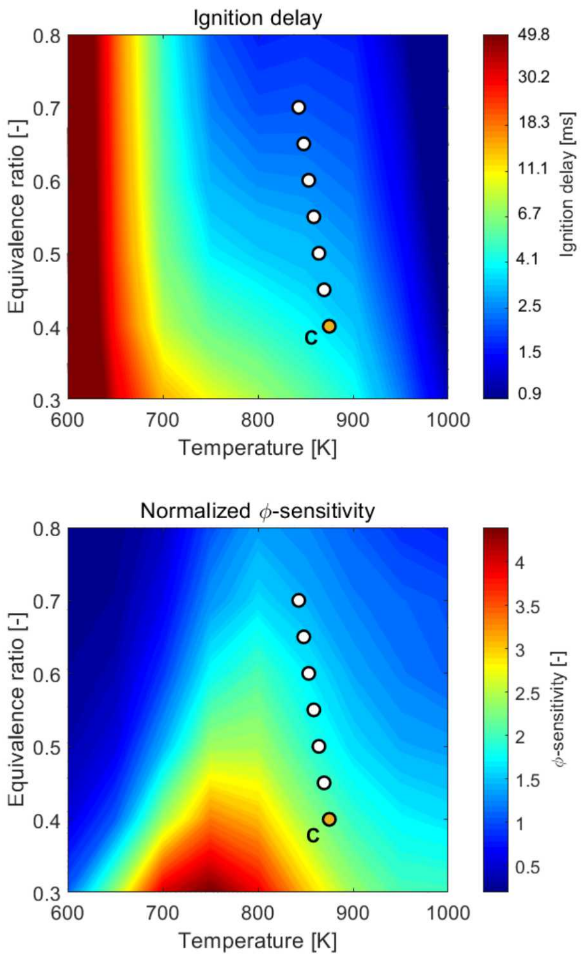

Figure 4. Ignition delay map (top) and normalized φ-sensitivity map (bottom) for iso-octane at P = 64.7 bar and X_{O2} = 21%.

Fuels that do not show NTC behavior

The same ignition delay and φ-sensitivity plots as the ones shown in the previous sub-section were also computed for the fuels defined in Table 2 that do not show a clear NTC zone. Fig. 5 shows the ignition delay and normalized φ-sensitivity of toluene in a pressure-vs-temperature map at $\varphi_m = 0.40$ and $X_{O2} = 21\%$. The φ-sensitivity remains almost constant for the whole map, which means that the φ-sensitivity is almost independent of pressure and temperature for fuels without NTC behavior (the φ-sensitivity is also found to be independent of the oxygen concentration). However, the normalized φ-sensitivity is inversely proportional to the equivalence ratio, i.e., the richer the mixture the lower the φ-sensitivity.

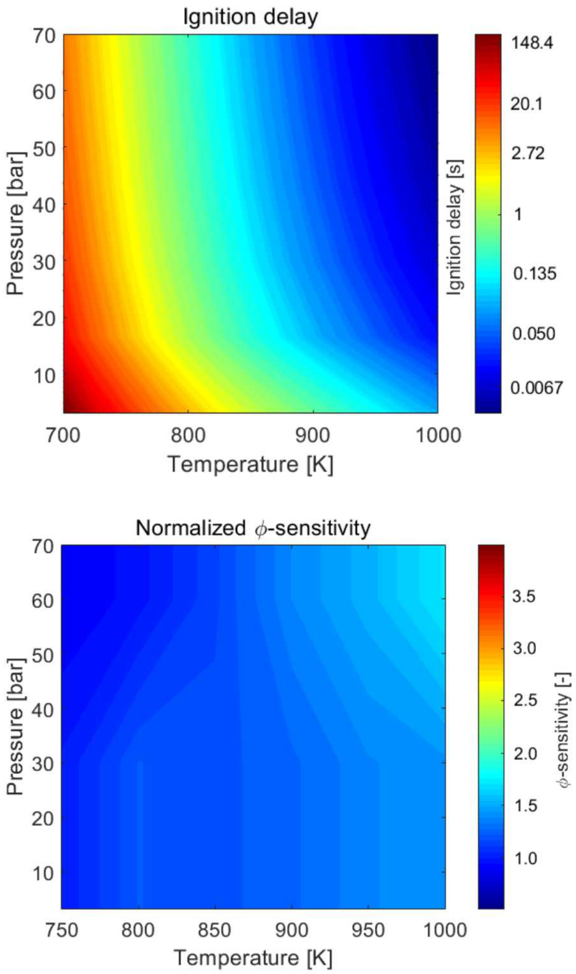

Figure 5. Ignition delay (top) and normalized φ-sensitivity (bottom) in a pressure vs temperature map for toluene at $\varphi_m = 0.40$ and $X_{O2} = 21\%$.

Comparing Fig. 2 –right with Fig. 5 – bottom, which have the same color scale, it can be seen that the maximum φ-sensitivity value is much lower for those fuels that do not show NTC behavior. In fact, the φ-sensitivity of fuels with NTC zone is higher than the φ-sensitivity of fuels without NTC zone even under the high-temperature regime. For instance, Fig. 2, right-hand plot, shows that the φ-sensitivity of iso-octane at point A (which represents the engine working at naturally aspirated conditions) and point C (which represents the engine working at high-boosted conditions) are equal to 1.63 and 2.03, respectively. However, the φ-sensitivity of toluene is equal to 1.38 and 1.25 under the same conditions. Therefore, fuels that show NTC behavior are highly desirable to increase the φ-sensitivity even if the working conditions are not characterized by a two-stage ignition.

Chemical kinetics behind the φ-sensitivity

Sensitivity analyses are performed in constant-volume reactors for the fuel species shown in Table 2, with the sensitivity coefficients of the different reactions calculated as described by Eq. 4. Simulations are carried out at three different temperatures that represent each of the different ignition regimes for the fuels that show NTC behavior, whereas only one temperature is evaluated for the fuels that do not have an NTC zone. Iso-octane and toluene are the fuels used to compute the results discussed in this sub-section. However, analogous results can be obtained with other fuels that do or do not show NTC behavior.

Fuels that show NTC behavior

Iso-octane is tested at 60 bar, $\varphi_m = 0.40$, $X_{O2} = 21\%$ and the following temperatures: 650 K (low-temperature regime), 800 K (NTC zone) and 950 K (high-temperature regime). Fig. 6 shows the sensitivity coefficients for the reactions that have the largest effect on the φ-sensitivity for each temperature regime. A sensitivity coefficient $\mathbf{S_i} > \mathbf{0}$ means that the φ-sensitivity increases if the specific reaction rate of reaction *i* increases, and $\mathbf{S_i} < \mathbf{0}$ means the φ-sensitivity decreases if the reaction rate increases. Thus, reactions that show high sensitivity coefficients in absolute value have a greater effect on the φ-sensitivity, but only reactions that show $\mathbf{S_i} > \mathbf{0}$ tend to improve this property. Also, the reader should note that high $\mathbf{S_i}$ values do not mean that the fuel is highly φ-sensitive, only that the φ-sensitivity is highly controlled by these reactions. For example, reaction R5 (IC8 + OH = IC8-4R + H2O) in Fig. 6 shows one of the largest $\mathbf{S_i}$ values; however, the φ-sensitivity of iso-octane is almost negligible at these low-temperature conditions (see Fig. 2 – right).

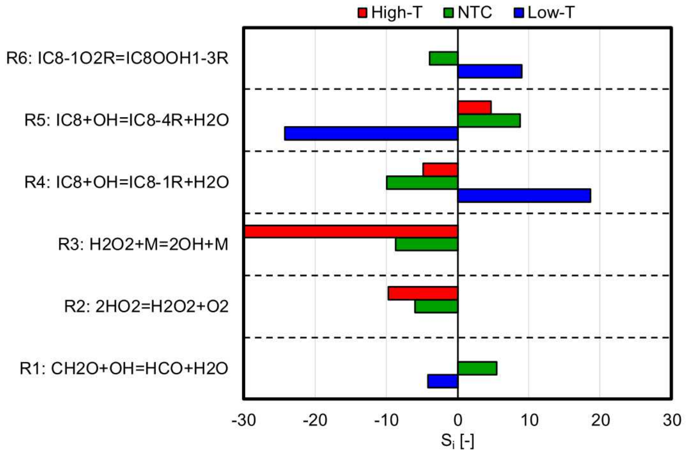

Figure 6. Sensitivity analyses for the φ-sensitivity of iso-octane at 60 bar, $\varphi_m = 0.40$ and $X_{O2} = 21\%$. Three different temperature regimes are tested.

For fuels exhibiting LTHR, ignition is controlled by the low-temperature chain branching mechanism at 650 K. The LTHR is mainly controlled by temperature and almost independent of pressure, equivalence ratio or oxygen content [36 – 38], which results in low φ-sensitivity values, since combustion is dominated by the LTHR. In this LTHR regime, iso-octane dehydrogenation reactions through OH (R4 and R5 in Fig. 6) are the reactions most responsible for the φ-sensitivity; however, their effect on the φ-sensitivity depends on the alkyl radical generated. Reaction R4 describes how the first carbon of iso-octane's chain loses a hydrogen, generating the alkyl radical IC8-1R. On the other hand, reaction R5 described how the fourth carbon of iso-octane's chain loses a hydrogen, generating the alkyl radical IC8-4R. Two different pathways compete in this regime: the low-temperature chain branching mechanism and β-scission reactions. The low-temperature chain branching mechanism generates active radicals that promote the ignition, contributing to the φ-sensitivity. Conversely, stable intermediate species are generated by β-scission reactions, leading to lower φ-sensitivity values. The decomposition of the alkyl radical IC8-1R (generated from reaction R4) is mainly controlled by the low-temperature mechanism, since its β-scission decomposition reaction only occurs at higher temperature (E_a = 8520 cal/mol). Thus, the φ-sensitivity increases if R4 is enhanced (Fig. 6 shows that the sensitivity coefficient of R4 is positive). However, the alkyl radical IC8-4R (generated from reaction R5) partially decomposes through β-scission even at low temperatures (E_a = 6130 cal/mol). Thus, the φ-sensitivity decreases if R5 is enhanced (Fig. 6 shows that the sensitivity coefficient of R5 is negative). In summary, the reactivity increases by enhancing the formation of IC8-1R, while it decreases if enhancing the formation of IC8-4R, causing an opposite effect on the φ-sensitivity. However, the φ-sensitivity values reached in this regime are low in any case.

The NTC regime, which has been linked to high φ-sensitivity values in Fig. 2, is reached at medium temperatures because β-scission reactions that are negligible during the low-temperature regime become relevant pathways. These reactions compete with the formation of active radicals by the low-temperature chain branching mechanism, decreasing the overall reactivity. The higher the temperature, the earlier and the less intense the LTHR, while the delay between the LTHR and the hot ignition (the characteristic time of the ITHR) increases, which means that the relevance of the ITHR also increases. Fig. 6 shows that the high φ-sensitivity values reached in the NTC regime are controlled by the generation of formyl radical by formaldehyde (R1: CH2O + OH = HCO + H2O), the generation of hydrogen peroxide (R2: 2HO2 = H2O2 + O2), and the decomposition of hydrogen peroxide (R3: H2O2 + M = 2OH + M). Chemical kinetic analyses also show that these reactions are primarily responsible for the heat released during the ITHR. Therefore, high φ-sensitivity values are controlled by ITHR reactions. The φ-sensitivity increases if R1 is enhanced (positive $\mathbf{S_i}$ value shown by R1 in Fig. 6). Formaldehyde and formyl radical, which are involved in R1, are species generated directly from the fuel and, therefore, they are highly sensitive to φ. Thus, the φ-sensitivity increases if formyl radical pathways are enhanced (R1). The φ-sensitivity decreases if the formation (R2) and decomposition (R3) of hydrogen peroxide is enhanced (negative $\mathbf{S_i}$ values shown by R2 and R3 in Fig. 6). The characteristic time of the ITHR is shortened if R2 and R3 are enhanced (faster transition from low-temperature to hot ignition), decreasing the relevance of the NTC zone and, therefore, decreasing the φ-sensitivity. Fig. 6 also shows that the formation of IC8-1R (R4) tends to decrease the φ-sensitivity during the NTC regime ($\mathbf{S_i} < \mathbf{0}$), whereas the formation of IC8-4R (R5) tends to enhance this property ($\mathbf{S_i} > \mathbf{0}$). The reader should notice that this is the opposite behavior of that seen for the low-temperature regime. β-scission reactions that cannot progress at low temperatures are now relevant. Thus, β-scission decomposition of the alkyl radical IC8-4R (generated from R5) promotes the NTC behavior, increasing the φ-sensitivity. Conversely, alkyl radical IC8-1R (generated from R4) promotes the low-temperature chain branching mechanism, decreasing the φ-sensitivity.

At high-temperature conditions, Fig. 6 shows that the φ-sensitivity is mainly controlled by the formation (R2) and decomposition (R3) of hydrogen peroxide at high-temperature conditions. As explained before, the φ-sensitivity decreased if R2 and R3 are enhanced because the transition between low-temperature and high-temperature ignition occurs faster. Finally, the higher the temperature, the more the ignition is controlled by the chemistry of hydrogen, which decreases the φ-sensitivity.

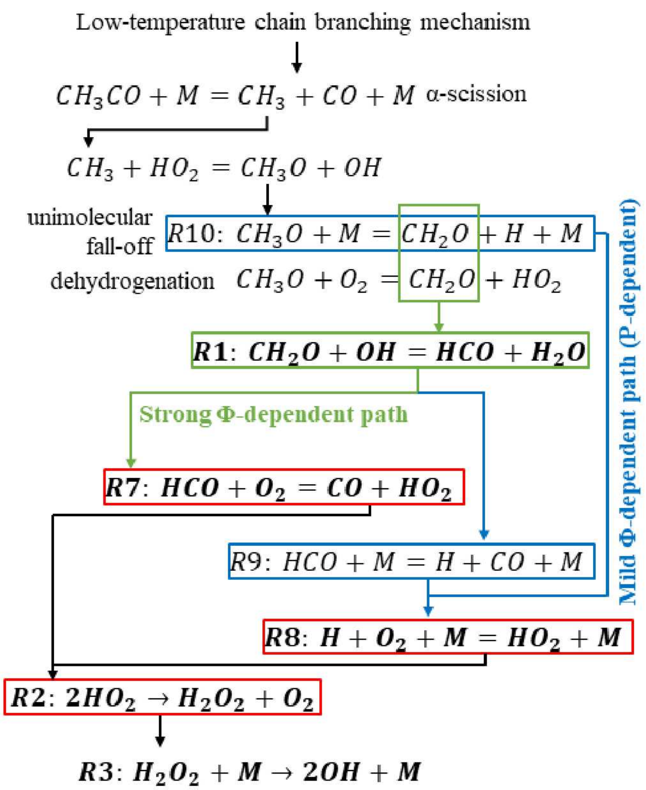

Figure 7. Schematic of the ITHR mechanism.

The main ITHR-producing reaction mechanism is shown in Fig. 7, in which reactions that contribute the most to the ITHR are outlined in red (R2, R7 and R8). This reaction mechanism represents the transition between low-temperature reactions and hot ignition. Two different pathways compete to each other, both of them contributing to the φ-sensitivity. First, the green pathway in Fig. 7 (R1 – R7 – R2) represents the strongly φ-dependent pathway, which is controlled by formyl radical reactions. Second, the blue pathway in Fig. 7 (R10 – R9 – R8 – R2) represents the mildly φ-dependent pathway, which is controlled by third-body reactions. Fig. 8 shows the φ-sensitivity evolution against temperature for iso-octane at two different pressures (30 bar and 60 bar), φ_m = 0.40 and X_{O2} = 21%. The operating conditions that are relevant for LTGC engines are outlined in the figure. Third-body reactions (R8, R9 and R10 in Fig. 7) are highly pressure-dependent and they become more relevant if the pressure increases, leading to higher H_2O_2 decomposition rates. This moves the NTC zone to higher temperatures, shifting the φ-sensitivity in temperature. Moreover, the higher the pressure, the more relevant the mild φ-dependent pathway (blue pathway in Fig. 7) at expense of the strong φ-dependent pathway (green pathway in Fig. 7), which reduces the φ-sensitivity peak value. However, increasing the pressure increases the overall φ-sensitivity under LTGC engine conditions. Point A in Fig. 8, which corresponds to point A in Fig. 2, represents an engine operating point under naturally aspirated conditions. If the intake pressure is increased (point B in Figs. 8 and 2) and the intake temperature is reduced to control the increasing reactivity (point C in Figs. 8 and 2), the φ-sensitivity increases. Therefore, the mildly φ-dependent pathway shown in Fig. 7

causes the high φ-sensitivity seen under high-boost engine-like conditions.

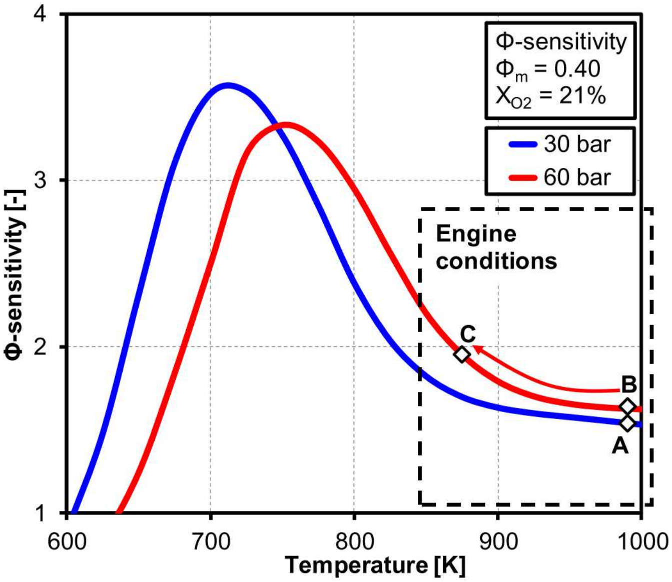

Figure 8. Evolution of the φ-sensitivity with temperature for two different pressures: 30 bar (blue) and 60 bar (red). Results from constant-volume reactor calculations at $\varphi_m = 0.40$ and $X_{O2} = 21\%$.

Fuels that do not show NTC behavior

Chemical kinetic simulations in constant-volume reactors are also performed for the fuel species in Table 2 that do not have NTC behavior. Sensitivity analyses are carried out at 60 bar, $\varphi_m = 0.40$, $X_{O2} = 21\%$ and 950 K, identifying the reactions that control the φ-sensitivity. The reader should notice that fuels without NTC behavior are characterized by low φ-sensitivity values, which are almost independent of pressure, temperature and oxygen content. Therefore, analyzing the chemical kinetics that cause the φ-sensitivity of non NTC fuels is not relevant for LTGC engines and only a brief explanation will be given.

The results with toluene show that the φ-sensitivity is mainly controlled by two groups of reactions. First, H abstraction reactions by molecular oxygen ($RH + O2 = R + HO2$) are the reactions most responsible for the φ-sensitivity of toluene. Second, oxygen addition to benzyl radicals, which is an intermediate species generated during toluene decomposition, by hydroperoxyl radicals ($C6H5CH2 + HO2 = C6H5CH2O + OH$) also controls the φ-sensitivity. The results with ethanol and di-iso-butylene show that fuel dehydrogenation is also the mechanism most responsible for the φ-sensitivity of these fuels. However, hydrogen peroxide decomposition (R3: $H2O2 + M = 2OH + M$) is found to also be partially responsible for the φ-sensitivity. However, despite the fact that fuel dehydrogenation reactions control the φ-sensitivity of fuels without NTC behavior, the φ-sensitivities of these fuels are very low and not relevant for LTGC engines.

Tailored Fuel Blends that Maximize the Φ-Sensitivity

Methodology: Designing tailored fuel blends

Tailored fuel blends are designed by modeling Sandia's LTGC/HCCI research engine in a 0-D, adiabatic, closed, internal combustion engine reactor (IC-engine) in CHEMKIN.

A surrogate fuel for a regular-grade, E10, RON 92, research-grade gasoline, known as RD5-87, is used to define the base condition at which the tailored fuel blends are designed. This surrogate, the formulation of which is described in Table 3, was developed by Sandia National Laboratories based on the actual fuel composition, and it has been validated against experimental results [39]. The molar fraction of each hydrocarbon class present in the fuel according to a detailed hydrocarbon analysis is also included in the table. Finally, the main properties of RD5-87 are shown in Table 6. The base condition is designed at an intake-boost pressure equal to 2.5 bar, which corresponds to the most reactive condition tested in this investigation. Experiments with RD5-87 show that the intake temperature cannot be decreased sufficiently to control the reactivity of the fuel when $P_{in} = 2.5$ bar [17]. Thus, the minimum BDC temperature allowable in Sandia's engine to avoid condensation phenomena in the intake system (see the *General Methodology* section), which is equal to 360 K, is imposed in the simulations. A global $\boldsymbol{\varphi_m}$ equal to 0.40 and an oxygen molar fraction equal to 12.6% (which corresponds to 58% EGR) are used at the base condition. The surrogate fuel for RD5-87 leads to a CA50 = 368.5 CAD under this operating condition. Therefore, the base condition is defined as follows:

- Intake pressure (P_{in}): 2.5 bar.
- BDC temperature (T_{BDC}): 360 K.
- Equivalence ratio (φ_m): 0.40.
- Oxygen molar fraction (X_{O2}): 12.6%.
- 50% burn point (CA50): 368.5 CAD.

Table 3. Sandia's surrogate formulation for RD5-87.

RD5-87		**Surrogate fuel**	
Hydrocarbon class	**Molar concentration**	**Species**	**Molar concentration**
N-paraffins	16.4 %	N-pentane	9.0 %
		N-heptane	9.0 %
Iso-paraffins	23.6 %	Iso-octane	29.0 %
Cyclo-paraffins	12.2 %	Cyclo-pentane	7.0 %
Aromatics	21.1 %	Toluene	20.0 %
Olefins	5.8 %	1-Hexene	6.0 %
Oxygenated	19.9 %	Ethanol	20.0 %

16 different single-component fuels (listed in Appendix A) are tested at the base condition, and they are classified as high-reactivity fuels (CA50 ≤ 368.5 CAD) or low-reactivity fuels (CA50 > 368.5 CAD). Then, 2-component blends are designed by mixing high- and low-reactivity fuels. The blend ratio is adjusted to match the autoignition of RD5-87 at the base condition (i.e., the most reactive condition), so the simulated CA50 = 368.5 CAD (±0.4 CAD) at this base point. Thus, all blends designed in this investigation show the same reactivity as

RD5-87 at this highest-boost condition (i.e., the most reactive condition), which ensures that the fuel blends are not too reactive to work in the engine.

Figure 9 graphically shows how a 2-component blend is designed. In this particular case, toluene (which is a low-reactivity fuel) is mixed with 1-hexene (which is a high-reactivity fuel) to match the reactivity of RD5-87 under the base conditions. The toluene / 1-hexene blend ratio is adjusted through an iterative process that ends when the combustion phasing shown by RD5-87 is replicated. Once the fuel blend is formulated, lower-boost pressures are simulated while keeping the CA50 constant and equal to 368.5 CAD (±0.4 CAD). To do so, the oxygen concentration is increased as the pressure is decreased, and once 0% EGR is reached, the combustion phasing is controlled by adjusting the BDC temperature. Using this procedure, both RD5-87 and the tailored fuel blends are tested at $P_{in} = 2.5$ bar (the base fuel-design conditions) and $P_{in} = 1.0$, 1.3, 1.6 and 2.0 bar. As shown in the *Φ-Sensitivity Fundamentals*, high φ-sensitivity values are easily obtainable at high-boosted conditions. The challenge consist of designing a fuel that has high φ-sensitivity under naturally aspirated conditions and sufficient autoignition resistance to work at high-boost conditions. Therefore, the φ-sensitivities of various 2-component fuel blends at $P_{in} = 1.0$ bar are used to select the most promising species to enhance this property.

The Research Octane Number (RON), Motor Octane Number (MON) and octane sensitivity (S = RON – MON) of a fuel blend are calculated by combining the blending octane numbers of the different species involved in the mixture as follows:

$$\boldsymbol{RON_{blend} = \sum BRON_j LVF_j} \quad \mathbf{(6)}$$

Where $BRON_j$ represents the blending RON of the species j, while LVF_j represents the liquid volume fraction of the species j in the mixture. An analogous form of Eq. 6 is used for calculating MON. BRON and BMON values are taken from the A.P.I. Research Project 45 [40].

The φ-sensitivity is evaluated using the pressure and temperature values under motored conditions (simulations with chemistry turned off) that correspond to the 10% burn point (CA10) for $\varphi_m = 0.40$ and $X_{O2} = 21\%$. The thermodynamic conditions corresponding to CA10 (P_{CA10} and T_{CA10}) are chosen because they represent the in-cylinder conditions at the start of ignition. The temperature variations relative to this T_{CA10} for $\varphi_m = 0.40$ that would result from an equivalence ratio distribution produced by a late-DI fuel-injection strategy (designed to produce charge-mixture stratification) are estimated by solving Eq. 2, which takes into account cooling effect caused by the heat of vaporization of the fuel for the various φ_m. As explained previously, the effects of the differences in specific-heat ratio with changes in φ_m (which can affect the temperature and pressure changes due to compression during the ignition delay), as well as the effects of heat losses, convection, and turbulence, are not taken into account. Therefore, in a real engine, the thermal stratification produced by mixture stratification is expected to be greater than the amount accounted for in these simulations.

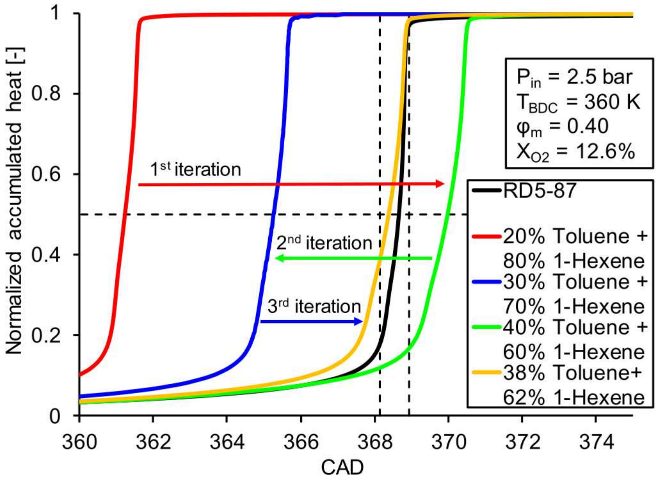

Figure 9. Iterative process to design 2-component fuel blends that replicate the reactivity of RD5-87 under base conditions.

This procedure is illustrated in Fig. 10, which shows how the φ-sensitivity is obtained under engine-like conditions for the example pressure of $P_{in} = 1.0$ bar. The plot at the left shows the in-cylinder temperature versus pressure evolution under motored conditions, in which the point that corresponds to CA10 at $\varphi_m = 0.40$ is shown as an

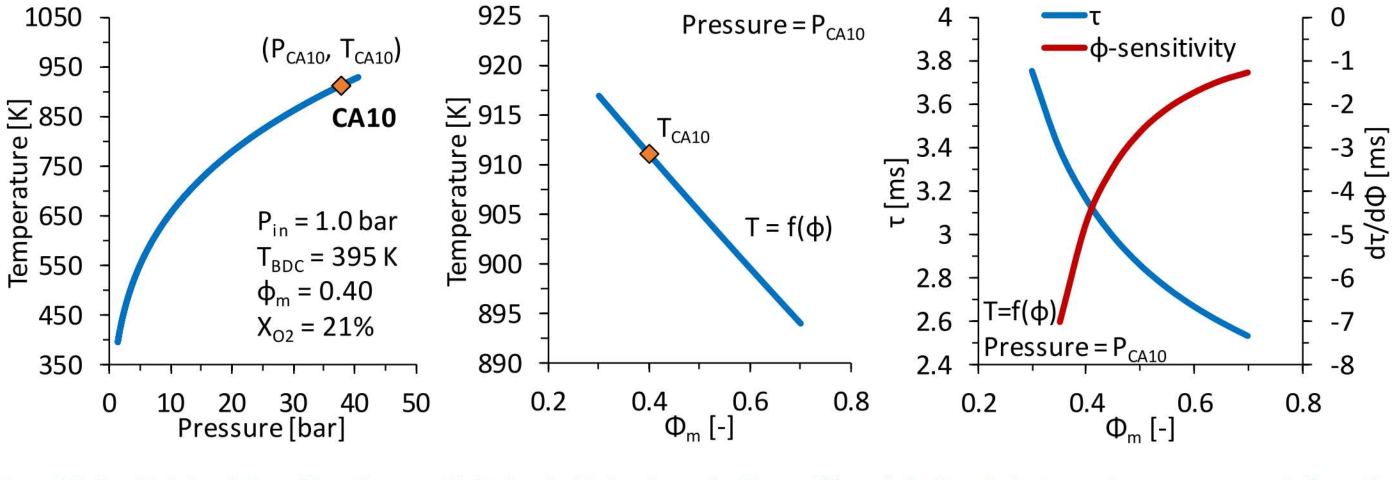

Figure 10. Graphical description of how the φ-sensitivity is calculated under engine-like conditions. Left.- In-cylinder temperature vs pressure evolution under motored conditions. Center.- Temperature distribution for a range of equivalence ratios that has been estimated by taking into account the heat of vaporization of the fuel. Right.- Ignition delay and φ-sensitivity for the temperature distribution shown in the central plot.

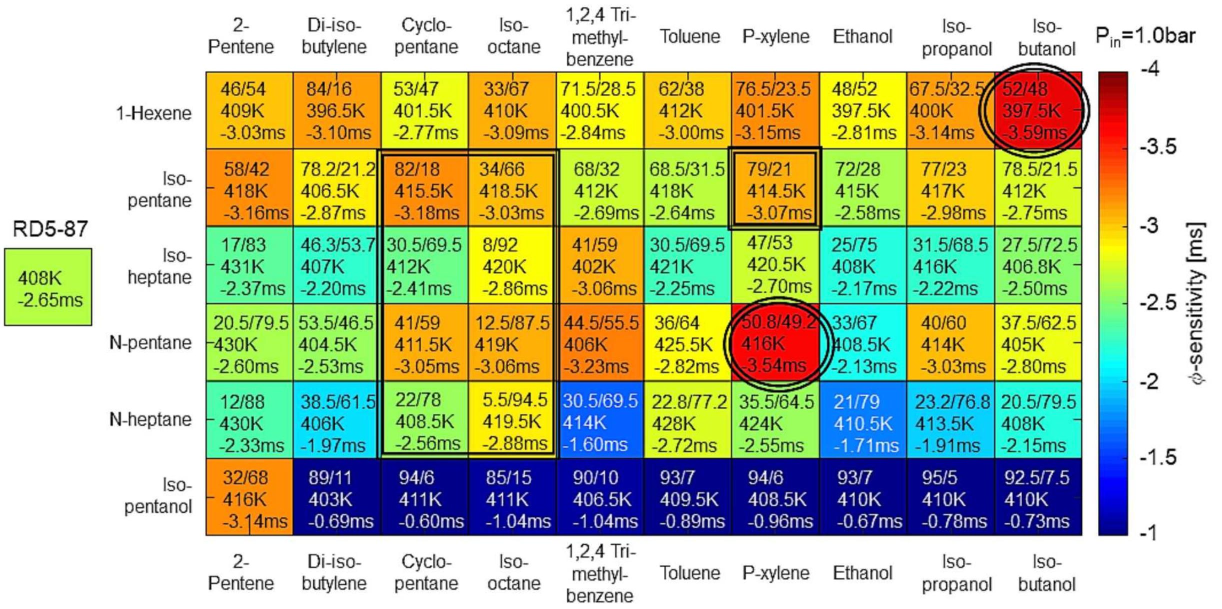

	2-Pentene	Di-iso-butylene	Cyclo-pentane	Iso-octane	1,2,4 Tri-methyl-benzene	Toluene	P-xylene	Ethanol	Iso-propanol	Iso-butanol
1-Hexene	46/54 409K -3.03ms	84/16 396.5K -3.10ms	53/47 401.5K -2.77ms	33/67 410K -3.09ms	71.5/28.5 400.5K -2.84ms	62/38 412K -3.00ms	76.5/23.5 401.5K -3.15ms	48/52 397.5K -2.81ms	67.5/32.5 400K -3.14ms	52/48 397.5K -3.59ms
Iso-pentane	58/42 418K -3.16ms	78.2/21.2 406.5K -2.87ms	82/18 415.5K -3.18ms	34/66 418.5K -3.03ms	68/32 412K -2.69ms	68.5/31.5 418K -2.64ms	79/21 414.5K -3.07ms	72/28 415K -2.58ms	77/23 417K -2.98ms	78.5/21.5 412K -2.75ms
Iso-heptane	17/83 431K -2.37ms	46.3/53.7 407K -2.20ms	30.5/69.5 412K -2.41ms	8/92 420K -2.86ms	41/59 402K -3.06ms	30.5/69.5 421K -2.25ms	47/53 420.5K -2.70ms	25/75 408K -2.17ms	31.5/68.5 416K -2.22ms	27.5/72.5 406.8K -2.50ms
N-pentane	20.5/79.5 430K -2.60ms	53.5/46.5 404.5K -2.53ms	41/59 411.5K -3.05ms	12.5/87.5 419K -3.06ms	44.5/55.5 406K -3.23ms	36/64 425.5K -2.82ms	50.8/49.2 416K -3.54ms	33/67 408.5K -2.13ms	40/60 414K -3.03ms	37.5/62.5 405K -2.80ms
N-heptane	12/88 430K -2.33ms	38.5/61.5 406K -1.97ms	22/78 408.5K -2.56ms	5.5/94.5 419.5K -2.88ms	30.5/69.5 414K -1.60ms	22.8/77.2 428K -2.72ms	35.5/64.5 424K -2.55ms	21/79 410.5K -1.71ms	23.2/76.8 413.5K -1.91ms	20.5/79.5 408K -2.15ms
Iso-pentanol	32/68 416K -3.14ms	89/11 403K -0.69ms	94/6 411K -0.60ms	85/15 411K -1.04ms	90/10 406.5K -1.04ms	93/7 409.5K -0.89ms	94/6 408.5K -0.96ms	93/7 410K -0.67ms	95/5 410K -0.78ms	92.5/7.5 410K -0.73ms

RD5-87
408K -2.65ms

Figure 11. Averaged φ-sensitivity at P_{in} = 1.0 bar for all the 2-component fuel blends tested in this investigation. The molar blend ratio between low- and high-reactivity fuels, the BDC temperature needed to obtain a CA50 = 368.5 CAD (±0.4 CAD) and the averaged φ-sensitivity value are also included for each case. The two most promising blends are encircled and the blends that meet U.S. regulation for formulation are squared. Results for RD5-87 are included in the left side of the figure.

orange diamond. At these conditions, Eq. 2 is applied to determine the changes in temperature that occur with stratification due to differences in vaporization cooling for the different equivalence-ratio regions. Assuming a fuel distribution from φ = 0.30 to φ = 0.70 at steps of 0.05 and applying Eq. 2 to each φ results in the temperature distribution plotted in Fig. 10 – center. Then, this temperature vs φ distribution is imposed in a closed homogeneous reactor under constant-volume conditions, to obtain an ignition delay value for each φ – T combination (Fig. 10 – right). Finally, the φ-sensitivity is calculated as shown by Eq. 3. This procedure was carried out at several intake pressures, first for RD5-87, and then for each potential fuel blend investigated.

Results and Discussion: Tailored Fuel Blends that Maximize the Φ-Sensitivity

To develop a fuel blend that increases the φ-sensitivity above that of RD5-87, the simplest case, 2-component blends are investigated first. These blends are designed by mixing the high- and low-reactivity fuels described in Appendix A. Mixing high- and low-reactivity species is necessary in order to obtain fuel blends with the appropriate reactivity. For each blend, the amount of each component (molar blend ratio) is adjusted to obtain CA50 = 368.5 CA at the base condition as explained with respect to Fig. 2 in the preceding subsection. Using this mixture, the φ-sensitivities at P_{in} = 1.0 bar are calculated for a range of equivalence ratios as shown by Fig. 3, with T_{BDC} adjusted to maintain CA50 = 368.5 CA. These φ-sensitivities at the various equivalence ratios are then averaged in order to obtain a single value that characterizes the φ-sensitivity of each fuel blend. This value for P_{in} = 1.0 bar is used to identify the most promising blends because the φ-sensitivity is weaker at lower pressures (see discussion with respect to Fig. 4).

The results of these evaluations at P_{in} = 1.0 bar for the 2-component blends are presented in the matrix in Fig. 11. Low-reactivity fuels are shown in the horizontal-axis and high-reactivity fuels are shown in the vertical-axis. The molar blend ratio between low- and high-reactivity fuels, the BDC temperature needed to properly phase the combustion (CA50 = 368.5 CAD ±0.4 CAD) and the averaged φ-sensitivity value are given for each case. The averaged φ-sensitivities are also indicated by the colors for more-rapid evaluation, with red indicating the highest φ-sensitivities. The reader should remember that the more negative the φ-sensitivity the more φ-sensitive is the fuel, since $d\tau/d\varphi < 0$. For instance, a mixture composed by $79\%_{mol}$ iso-pentane and $21\%_{mol}$ p-xylene needs T_{BDC} = 414.5 K to properly ignite at P_{in} = 1.0 bar, φ_m = 0.40 and X_{O2} = 21%; and the averaged φ-sensitivity at P_{in} = 1.0 bar is equal to -3.07 ms. Because the blend ratio has been adjusted to replicate the reactivity of the regular E10 gasoline (RD5-87) at the most reactive condition tested in this investigation (P_{in} = 2.5 bar), all the blends designed in this work can be run in Sandia's LTGC engine without surpassing the engine limits in terms of minimum intake temperature and maximum EGR rate. Results for RD5-87 are included in the left side of the figure to ease the evaluation of the blends.

In general, fuels ignite in the high-temperature regime for P_{in} = 1.0 bar. Thus, fuels whose NTC behavior occurs at high temperatures are more likely to have high φ-sensitivity values at this P_{in}, because the operating conditions will be closer to the NTC zone. N-alkanes and short-chain olefins show hotter NTC zones than iso-alkanes. For example, the low-temperature side of the NTC zone ≈800 K for 1-hexene, n-pentane and n-heptane versus ≈700 K for iso-octane at φ_m = 0.40, X_{O2} = 21%, and 30 bar (the nominal TDC pressure for P_{in} = 1.0 bar). Therefore, n-alkanes and short-chain olefins are, theoretically, the most promising hydrocarbon classes to design a fuel blend with high φ-sensitivity at P_{in} = 1.0 bar. However, n-heptane results in Fig. 11 seem to contradict this statement, since they show relatively low φ-sensitivity values. The reason why the φ-sensitivity is low for these n-heptane blends is because large concentrations of low-reactivity fuel are required to balance the very high reactivity of n-heptane. Low-reactivity fuels usually do not show NTC behavior and are characterized by low φ-sensitivity values, decreasing the overall φ-sensitivity of the mixture. This effect is less relevant when using n-pentane because this species is less reactive than n-heptane. Thus, less of the low-reactivity component is required, and the higher blend ratio of n-alkane results in higher φ-sensitivity. In fact, the fuel blend that consists of $51\%_{mol}$ n-pentane + $49\%_{mol}$ p-xylene shows one of the highest φ-sensitivity values.

1-Hexene blends are the most φ-sensitive mixtures, supporting the idea that short-chain olefins tend to increase the φ-sensitivity. In fact, $52\%_{mol}$ 1-hexane + $48\%_{mol}$ iso-butanol is the most promising 2-component blend tested in this investigation. It should be noted that short-olefin + iso-alcohol blends lead to high φ-sensitivity, because iso-alcohols inhibit the NTC zone of short-chain olefins to a lesser extent than other hydrocarbon classes (especially aromatics). For instance, iso-pentanol blends show the lowest φ-sensitivity values among all the blends tested except for the mixture with 2-pentene, which is very φ-sensitive. Long-chain, branched olefins, such as di-iso-butylene, are characterized by low reactivities and almost negligible NTC behavior, leading to low φ-sensitivities. Therefore, the effect of short-chain and long-chain, branched olefins on φ-sensitivity should not be confused with each other.

Table 4. U.S. regulation for composition of regular gasolines.

Species	Max vol. frac. [%]
Olefins	17.5
Aromatics	30.4
Ethanol	10.0
Iso-butanol	16.0

Table 5. Formulation in molar base of the two most promising 2-component fuel blends (Blend #1 and Blend #2). The two multi-component tailored fuel blends designed in this investigation (Blend #3 and Blend #4) are also included in the table.

Species	Blend #1	Blend #2	Blend #3	Blend #4
N-pentane	-	50.8%	29.0%	28.5%
Iso-octane	-	-	-	8.0%
Cyclo-pentane	-	-	7.5%	-
P-xylene	-	49.2%	30.0%	30.0%
1-Hexene	52.0%	-	17.5%	17.5%
Iso-butanol	48.0%	-	16.0%	16.0%

The U.S. regulation for composition of regular gasolines is shown in Table 4. 2-component blends that meet this regulation are marked in Fig. 11 with a square or rectangle around the cells. It can be seen that legally marketable fuel blends that are more φ-sensitive than RD5-87 at P_{in} = 1.0 bar can be defined. However, realistic gasoline blends should meet two additional technical requirements. First, the blends must be also suitable fuels for standard spark ignition (SI) engines, since a transition from LTGC mode to SI mode may be required to reach high engine loads (i.e. for mixed-mode engines). Also, it would be very difficult to introduce a new gasoline into the market that did not work well for SI engines as well as LTGC, and even for full-time LTGC, the high load will be limited if the fuel becomes too reactive with intake boost [11, 38]. Thus, practical fuel blends must show high RON and octane-sensitivity values as well as high φ-sensitivity. Second, the BDC temperature required to ignite the mixture at P_{in} = 1.0 bar (the most difficult condition) must be similar to or lower than the temperature required for a regular gasoline. BDC temperature is controlled in LTGC engines by several techniques such as retaining hot residuals, NVO fuel injection, or intake heating using the engine coolant or exhaust gases. The higher the required temperature, the more complex the application of these techniques. Despite the fact that all the 2-component mixtures in Fig. 11 have high RON values, blends that include iso-alkanes show lower octane-sensitivities than RD5-87. The blend composed by $41\%_{mol}$ n-pentane + $59\%_{mol}$ cyclo-pentane is the only one that meets all the legal requirements and has a φ-sensitivity = -3.05 ms at P_{in} = 1.0 bar that is 15% more than that of RD5-87, RON = 95.0, octane-sensitivity = 11.2.

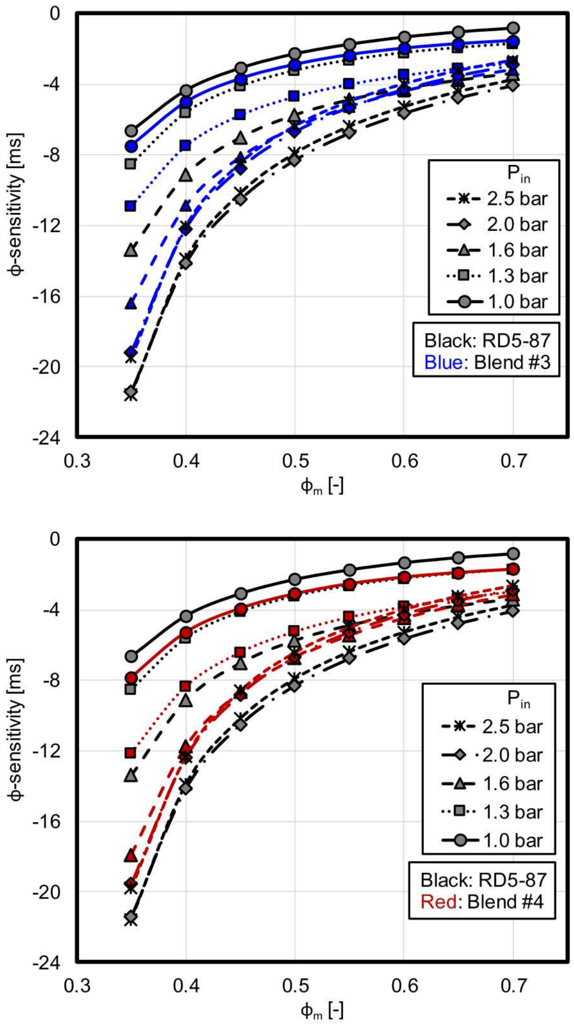

Figure 12. Φ-sensitivity for RD5-87 and two multi-component fuel blends at several intake pressures. Top.- Blend #3. Bottom.- Blend #4.

The 2-component fuel blends showing the highest φ-sensitivities in Fig. 11 are indicated by the circles around their red-colored cells. Blend #1 corresponds to the highest φ-sensitivity with oxygenated species ($52\%_{mol}$ 1-hexene + $48\%_{mol}$ iso-butanol), whereas Blend #2 corresponds to the highest φ-sensitivities without oxygenated species ($50.8\%_{mol}$ n-pentane + $49.2\%_{mol}$ p-xylene). However, the concentrations of some of the species in these mixtures exceed the maximum allowable by U.S. regulations, as shown in Table 4. To develop blends that meet current regulations and provide higher φ-sensitivities, RONs, and octane-sensitivities than RD5-87, multi-component blends are examined. Tests of multiple mixture

Table 6. Main properties of RD5-87, Blend #1 and Blend #2. RON and MON values for Blend #1 and Blend #2 are estimated by Eq. 6.

	RD5-87	**Blend #1**	**Blend #2**	**Blend #3**	**Blend #4**
Chemical formula	$C_{6.01}H_{11.84}O_{0.20}$	$C_{5.04}H_{11.04}O_{0.48}$	$C_{6.48}H_{11.02}O_{0.00}$	$C_{5.92}H_{10.93}O_{0.16}$	$C_{6.16}H_{11.56}O_{0.16}$
H/C ratio	1.972	2.190	1.701	1.848	1.878
O/C ratio	0.033	0.095	0.000	0.027	0.026
Air/Fuel stoich. ratio	14.018	13.164	14.346	13.987	14.052
Molecular weight	87.99 g/mol	79.20 g/mol	88.73 g/mol	84.47 g/mol	87.98 g/mol
Density	749 kg/m^3	725 kg/m^3	746 kg/m^3	742 kg/m^3	736 kg/m^3
RON	92.1	100.2	104.7	101.5	101.5
MON	84.8	86.4	95.0	88.3	90.0
AKI	88.5	93.3	99.8	94.9	95.8
Octane-sensitivity	7.3	13.8	9.7	13.1	11.5
T_{BDC} at P_{in} = 1.0 bar	408 K	397.5 K	416 K	406.2 K	407.5 K

combinations showed that the most promising results were obtained by mixing 17.5% 1-hexene, 16% iso-butanol, 30% p-xylene (the legal limits for these compounds) with variable amounts of n-pentane and a low-reactivity component to balance the reactivity. The blending ratio between n-pentane and the low-reactivity fuel is adjusted to replicate the reactivity of RD5-87 at P_{in} = 2.5 bar, as discussed in the previous subsection. Two different low-reactivity species, cyclo-pentane and iso-octane, are used to define Blend #3 and Blend #4, respectively. These species are chosen because cyclo- and iso-alkanes are the only hydrocarbon classes that can be used to control the reactivity that are not limited by U.S. regulations. The formulations for Blends #1 through #4 are shown in Table 5.

Figure 12 shows the φ-sensitivity at several intake pressures calculated as explained in the discussion of Fig. 3. Blend #3 and Blend #4 are compared with RD5-87 in Fig. 12 – top and Fig. 12 – bottom, respectively. The reader should remember that the more negative the φ-sensitivity the more φ-sensitive is the fuel, since $d\tau/d\varphi < 0$. It can be seen that the φ-sensitivities of the tailored fuel blends are significantly greater than those of RD5-87 at low and medium pressures. Blend #4 gives the best performance with averaged φ-sensitivity improvements of 34%, 56% and 20% at P_{in} = 1.0 bar, 1.3 bar and 1.6 bar, respectively. Both Blend #3 and Blend #4 have lower φ-sensitivity than RD5-87 at $P_{in} \geq 2.0$ bar; however, this is not considered important since the φ-sensitivity is still quite high for these P_{in}s. In general, most fuels have φ-sensitivity values at high pressures that are sufficiently high to obtain the benefits associated with the various forms of fuel stratification, as discussed in the Introduction. Table 6 shows the main properties of RD5-87 and Blends #1 – #4. The tailored fuel blends proposed in this investigation not only have higher φ-sensitivity values at low and medium pressures than RD5-87, but also higher RON, MON and octane-sensitivity. In fact, Blend #3 and Blend #4 are premium gasolines according to their anti-knock indexes, and with their high RON and octane-sensitivity values they are suitable fuels even for advanced, high-boost spark ignition engines. Also importantly, the reactivities of Blend #3 and Blend #4 are similar to that of RD5-87 at P_{in} = 1.0 bar, φ_m = 0.40 and X_{O2} = 21% (i.e., a similar BDC temperature is needed to obtain the same combustion phasing), which means that obtaining autoignition at lower loads in LTGC and spark-assisted LTGC engines would require no more effort than for regular gasoline, unlike some premium-grade gasolines

The overall changes in φ-sensitivity shown in Fig. 12 for blends #3 and #4 are more easily visualized in the bar graph in presented in Fig. 13. This figure shows the averaged φ-sensitivity at each pressure for RD5-87 and Blends #1 – #4. All four of the tailored fuel blends proposed in this investigation improve the φ-sensitivity compared to RD5-87 at low and medium intake pressures where the fuels are less φ-sensitive. At high pressures the tailored blends give lower φ-sensitivities than RD5-87, but this is inconsequential since the values are still quite high. More specifically, the φ-sensitivity increases approx. 32%, 52% and 14% at 1.0 bar, 1.3 bar and 1.6 bar, respectively, while it decreases approx. 17% at 2.0 bar and 2.5 bar. The φ-sensitivity increases with intake pressure up to P_{in} = 2.0 bar because BDC temperature is used to control the reactivity of the mixture, and the temperature is reduced as P_{in} is increased shifting the autoignition conditions closer to the NTC region (see Fig. 4 – right). However, similar φ-sensitivity values are reached at both 2.0 bar and 2.5 bar because EGR is used to balance the changes in reactivity with P_{in}, and P_{in} and EGR rate have opposite effects on φ-sensitivity (see Fig. 5). It can be seen that at P_{in} = 1.0 bar, the φ-sensitivity of Blend #4, which is the most φ-sensitive blend that meets the U.S. regulations for composition, is as high as the φ-sensitivity of Blend #1, which has the highest φ-sensitivity of the 2-component fuel blends that were designed no limitations on composition. Furthermore, at P_{in} =1.3 and 1.6 bar, the φ-sensitivity of Blend #4 exceeds that of Blend #1. These results show that market fuels that have high φ-sensitivities at lower P_{in}s can be designed using only relatively well-known species at legal concentrations (i.e. special uncommon species or concentrations beyond current legal limits are not required).

Despite the fact that Blend #4 is a legal marketable fuel from a point of view of formulation, actual market gasolines are composed of thousands of species, so the gasoline composition should be defined in terms of hydrocarbon classes. Thus, Blend #4 would correspond with a market gasoline composed by 17.5% short-chain olefins, 16% iso-butanol, 30% aromatics and a mixture of short-chain n-alkanes and long-chain iso-alkanes that leads to the desired reactivity or RON value (unleaded, plus or premium). According to the results obtained in this work, this market gasoline would show high φ-sensitivity and high octane-sensitivity. As such, it would be a suitable fuel for LTGC, SI, or mixed-mode (LTGC + SI) engines.

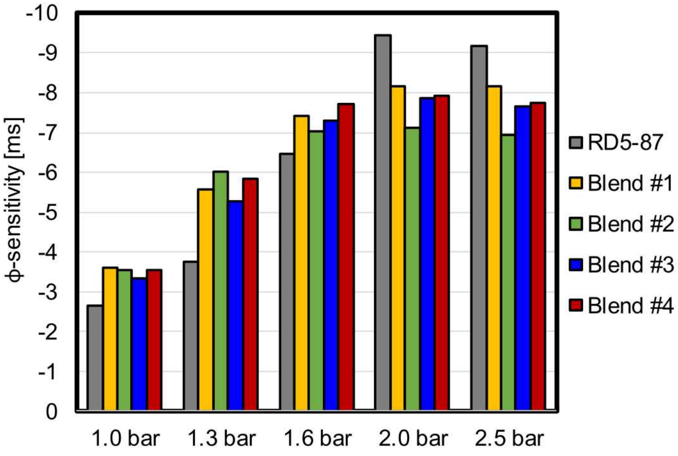

Figure 13. Averaged φ-sensitivity values at several intake pressures for RD5-87 and Blends #1 to #5.

Summary and Conclusions

The φ-sensitivity and the associated increase in ITHR offer substantial benefits for LTGC engines. Sequential autoignition is promoted by fuel stratification if the fuel is φ-sensitive, reducing the HRR peak and allowing higher loads without knock and/or CA50 to be advanced for higher efficiencies. Furthermore, if the fuel is φ-sensitive the CA50 can be controlled by the late-DI timing of a multiple-injection strategy. Finally, enhanced ITHR extends the allowable CA50 retard and improves stability.

The effects of the operating conditions on the φ-sensitivity and the chemical kinetics responsible for this phenomenon are analyzed in this article. To do so, the autoignition characteristics of 8 single-component fuels are obtained by means of numerical simulations carried out in CHEMKIN with a detailed chemical kinetic mechanism. These results are used to develop an understanding of the fundamentals of φ-sensitivity, and they show that φ-sensitivities are strongest for fuels capable of exhibiting NTC behavior. Later, the fuel matrix is extended to 16 different species that represent the different hydrocarbon classes usually found in gasolines. From these 16 species, tailored fuel blends are designed to improve the φ-sensitivity at low and medium intake pressures, with the restriction that they match the reactivity of a regular E10 gasoline (RD5-87) under high-boosted conditions (P_{in} = 2.5 bar) to ensure that autoignition reactivity remains within the same range. High φ-sensitivity, RON and octane-sensitivity values can be reached using 5-component fuel blends that also meet the U.S. regulations for the maximum concentrations of the various hydrocarbon classes. These results show that suitable market gasolines can be designed that will perform well for both LTGC and SI operation. The following conclusions are deduced from this investigation:

Regarding φ-sensitivity fundamentals:

- φ-sensitivity is strongest for fuels capable of exhibiting NTC behavior, but it is not necessary to operate in the central NTC region to obtain sufficient φ-sensitivity.
- The φ-sensitivity is greatest in the NTC region, reaching a maximum on the cold-side of the NTC. Increased φ-sensitivity in NTC region is due to enhanced ITHR reactions, which explains the experimental correlation between φ-sensitivity and ITHR.
- The φ-sensitivity decreases more gradually toward the hot side of the NTC region, and it remains at significant values during the transition between the NTC and high-temperature regimes and into the first part of the high-temperature region. This is of particular interest for LTGC combustion because autoignition often occurs in these regions for typical gasoline fuels.
- As autoignition shifts further into the high-temperature regime, ITHR, fuel-dependent reactions become less relevant and the ignition is more controlled by hydrogen chemistry typical of high-temperatures.
- Under naturally aspirated LTGC-engine conditions, the fuel usually ignites in the high-temperature regime. If the intake pressure is increased, the enhanced reactivity requires lower intake temperatures. Both higher intake pressures and lower intake temperatures act to increase the φ-sensitivity.
- If EGR is used to compensate for the increased reactivity as the intake pressure is increased, the reduced oxygen concentration has opposite effect of pressure on the φ-sensitivity, and the φ-sensitivity remains almost constant.
- For fuels that do not show NTC behavior, the φ-sensitivity is lower than for NTC fuels, and it is almost constant with changes in operating condition.

Regarding tailored fuel blends that improve φ-sensitivity:

- Short-chain olefins and n-alkanes are the most promising hydrocarbon classes to improve the φ-sensitivity because their NTC zones are located close to the typical autoignition temperatures in LTGC engines. However, these compounds are too reactive to be used as single-component fuels.
- Aromatics and iso-alcohols are the most promising species to control the reactivity of the fuel blends because of their high blending RON values and their high octane-sensitivities. Thus, combinations of short-chain olefins and n-alkanes with aromatics and iso-alcohols offer strong potential for forming φ-sensitive blends that also have high RON and high octane-sensitivity.
- Although binary mixtures of these two classes of compounds are capable of producing fuels with the desired combustion properties (high values of φ-sensitivity, RON, and octane-sensitivity), they cannot also meet the U.S. regulations for the maximum olefin, aromatic and iso-butanol content. Multiple-component blends are required to meet all the requirements.
- A 5-component fuel blend consisting of 17.5% 1-hexene (short-chain olefins), 16% iso-butanol, 30% p-xylene (aromatics), 28.5% n-pentane (short-chain n-alkanes) and 8% iso-octane (long-chain iso-alkanes) has been shown to be the most promising blend for enhancing the φ-sensitivity at low and medium intake pressures. The fuel blend also shows substantially higher RON (101.5) and octane-sensitivity (11.5) than a regular E10 gasoline, meaning that it is a suitable fuel for both LTGC and advanced SI engines. Furthermore, this mixture meets the U.S. regulations for formulation. Therefore, this investigation shows that market fuels can be designed that meet the requirements of LTGC, conventional SI, and advanced high-boost SI engines, or mixed-mode engines using a combination of LTGC and SI combustion.

References

1. Dec, J. E., "Advanced compression-ignition engines - understanding the in-cylinder processes," *Proceedings of the Combustion Institute*, 32:2727-2742, 2009.
2. Dec, J. E., "Advanced Compression-Ignition Combustion for High Efficiency and Ultra-Low NO_X and Soot," Encyclopedia of Automotive Engineering, John Wiley & Sons, 2014.

3. Zhao, F., Assanis, D. N., Asmus, T. N., Dec, J. E., Eng, J. A. and Najt, P. M., Homogeneous Charge Compression Ignition (HCCI) Engines, SAE International, 2003.
4. Kamimoto, T. and Bae, M., "High combustion temperature for the reduction of particulate in diesel engines," SAE Technical Paper 880423, 1988.
5. Olsson, J.-O., Tunestål, P., Johansson, B., Fiveland, S., Agama, J. R. and Assanis, D. N., "Compression Ratio Influence on Maximum Load of a Natural Gas-Fueled HCCI Engine," SAE paper 2002-01-0111, 2002.
6. Sjöberg, M., Dec, J. E., Babajimopoulos, A. and Assanis, D., "Comparing Enhanced Natural Thermal Stratification against Retarded Combustion Phasing for Smoothing of HCCI Heat-Release Rates," *SAE Transactions*, 113(3): 1557-1575, SAE paper 2004-01-2994, 2004.
7. Dec, J. E., Hwang, W. and Sjöberg, M., "An Investigation of Thermal Stratification in HCCI Engines Using Chemiluminescence Imaging," SAE Technical Paper 2006-01-1518, 2006.
8. Dec, J. E. and Hwang, W., "Characterizing the Development of Thermal Stratification in an HCCI Engine Using Planar-Imaging Thermometry," *SAE Int. J. Engines*, 2(1): 421-438, paper 2009-01-0650, 2009.
9. Dronniou, N. and Dec, J. E., "Investigating the Development of Thermal Stratification from the Near-Wall Regions to the Bulk-Gas in an HCCI Engine with Planar Imaging Thermometry," *SAE Int. J. Engines* 5(3): 1046-1074, 2012, SAE paper 2012-01-1111.
10. Kaiser, S. A., Schild, M. and Schulz, C., "Thermal stratification in an internal combustion engine due to wall heat transfer measured by laser-induced fluorescence," *Proceedings of the Combustion Institute*, 34:2911-2919, 2013.
11. Sjoberg, M., Dec, J. E. and Cernansky, N. P., "Potential of thermal stratification and combustion retard for reducing pressure-rise rates in HCCI engines, based on multi-zone modeling and experiments," SAE Technical Paper 2005-01-0113, 2005.
12. Kodavasal, J., Lavoie, G. A., Assanis, D. N. and Martz, J. B., "The effects of thermal and compositional stratification on the ignition and duration of homogeneous charge compression ignition combustion," *Combustion and Flame*, 162:451-461, 2015.
13. Kakuho, A., Nagamine, M., Amenomori, Y., Urushihara, T. and Itoh, T., "In-Cylinder Temperature Distribution Measurement and Its Application to HCCI Combustion," SAE Technical Paper 2006-01-1202, 2006.
14. Yang, Y., Dec, J. E., Dronniou, N. and Sjoberg, M., "Tailoring HCCI heat release rates with partial fuel stratification: comparison of two-stage and single-stage ignition fuels," *Proceedings of the Combustion Institute*, 33:3047-3055, 2011.
15. Yang, Y., Dec, J. E. and Dronniou, N., "Boosted HCCI combustion using low-octane gasoline with fully premixed and partially stratified charges," SAE Technical Paper 2012-01-1120, 2012.
16. Sjöberg, M. and Dec, J. E., "Comparing Late-cycle Autoignition Stability for Single- and Two-Stage Ignition Fuels in HCCI Engines," *Proceedings of the Combustion Institute*, 31: 2895–2902, 2007.
17. Dec, J. E. and Yang, Y., "Boosted HCCI for high power without engine knock and with ultra-low NOx emissions using conventional gasoline," SAE Technical Paper 2010-01-1086, 2010.
18. Sjöberg, M. and Dec, J. E., "Smoothing HCCI heat-release rates using partial fuel stratification with two-stage ignition fuels," SAE Technical Paper 2006-01-0629, 2006.
19. Dec, J. E. and Sjöberg, M., "Isolating the effects of fuel chemistry on combustion phasing in an HCCI engine and the potential of fuel stratification for ignition control," SAE Technical Paper 2004-01-0557, 2004.
20. Dec, J. E., Yang, Y. and Dronniou, N., "Boosted HCCI - controlling pressure-rise rates for performance improvements using partial fuel stratification with conventional gasoline," SAE Technical Paper 2011-01-0897, 2011.
21. Marriott, C. D. and Reitz, R. D., "Experimental investigation of direct injection-gasoline for premixed compression ignited combustion phasing control," SAE Technical Paper 2002-01-0418, 2002.
22. Kalghatgi, G. T., Risberg, P. and Angstrom, H.-E., "Partially pre-mixed auto-ignition of gasoline to attain low smoke and low NOx at high load in a compression ignition engine and comparison with a diesel fuel," SAE Technical Paper 2007-01-0006, 2007.
23. Yang, Y., Dec, J. E., Dronniou, N., Sjoberg, M. and Cannella, W., "Partial fuel stratification to control HCCI heat release rates: Fuel composition and other factors affecting pre-ignition reactions of two-stage ignition fuels," SAE Technical Paper 2011-01-1359, 2011.
24. Wada, Y. and Senda, J., "Demonstrating the potential of mixture distribution control for controlled combustion and emissions reduction in Premixed Charge Compression Ignition engines," SAE Technical Paper 2009-01-0498, 2009.
25. Dahl, D., Andersson, M., Berntsson, A., Denbratt, I. and Koopmans, L., "Reducing pressure fluctuations at high loads by means of charge stratification in HCCI combustion with negative valve overlap," SAE Technical Paper 2009-01-1785, 2009.
26. Mehl, M., Pitz, W., Sarathy, M., Yang, Y. and Dec, J. E., "Detailed kinetic modeling of conventional gasoline at highly boosted conditions and the associated intermediate temperature heat release," SAE Technical Paper 2012-01-1109, 2012.
27. Lee, K., Cho, S., Kim, N. and Min, K., "A study on combustion control and operating range expansion of gasoline HCCI," *Energy*, 91:1038-1048, 2015.
28. Li, C., Yin, L., Shamun, S., Tuner, M., Johansson, B., Solsjo, R. and Bai, X.-S., "Transition from HCCI to PPC: the sensitivity of combustion phasing to the intake temperature and the injection timing with and without EGR," SAE Technical Paper 2016-01-0767, 2016.
29. Shen, M., Tuner, M., Johansson, B., Tunestal, P. and Pagels, J., "Influence of injection timing on exhaust particulate matter emissions of gasoline in HCCI and PPC," SAE Technical Paper 2016-01-2300, 2016.
30. Gentz, G., Dec, J. E., Lopez-Pintor, D., Ji, C. and Dernotte, J., "Combustion-Timing Control of Low-Temperature Gasoline Combustion (LTGC) Engines by Using Double Direct-Injections to Control Kinetic Rates," SAE Technical Papers, in press, 2019.
31. Vedharaj, S., Vallinayagam, R., An, Y., Najafabadi, M. I., Somers, B., Chang, J. and Johansson, B., "Combustion Homogeneity and Emission Analysis during the Transition from CI to HCCI for FACE I Gasoline," SAE Technical paper no. 2017-01-2263, 2017.
32. Sellnau, M., et al., "GDCI Multi-Cylinder Engine for High Fuel Efficiency and Low Emissions," *SAE International Journal of Engines*, 2015. 8(2): p. 775-790.
33. Mehl, M., Pitz, W., Westbrook, C. K. and Curran, H. J., "Kinetic modeling of gasoline surrogate components and mixtures under engine conditions," *Proceedings of the Combustion Institute*, 33:193-200, 2011.
34. Mehl, M., Pitz, W., Westbrook, C. K., Yasunaga, K., Conroy, C. and Curran, H. J., "Autoignition behavior of unsaturated hydrocarbons in the low and high temperature regions," *Proceedings of the Combustion Institute*, 33:201-208, 2011.

35. Desantes, J. M., López, J. J., Molina, S. and López-Pintor, D., "Design of synthetic EGR and simulation study of the effect of simplified formulations on the ignition delay of isooctane and n-heptane," *Energy Conversion and Management*, 96:521-531, 2015.
36. Kumar, K., Mittal, G. and Sung, C.-J., "Autoignition of n-decane under elevated pressure and low-to-intermediate temperature conditions," *Combustion and Flame*, 156:1278-1288, 2009.
37. Kumar, K. and Sung, C.-J., "An experimental study of the autoignition characteristics of conventional jet fuel-oxidizer mixtures: Jet-A and JP-8," *Combustion and Flame,* 157:676-685, 2010.
38. Weber, B. W., Kumar, K., Zhang, Y. and Sung, C.-J., "Autoignition of nbutanol at elevated pressure and low-to-intermediate temperature," *Combustion and Flame*, 158:809-819, 2011.
39. López-Pintor, D., Dec, J. E. and Gentz, G., "An alternative surrogate fuel for an AKI 88.5 - E10 research-grade gasoline: Designing a methodology to replicate HCCI engine conditions in a single-zone model and validating the surrogate formulation versus experimental measurements," To be submitted.
40. Hydrocarbon Research Project from American Petroleum Institute and Research Project 45 from Ohio State University. "A.P.I. research project 45, Volume 1," American Petroleum Institute Hydrocarbon Research Project, the Ohio State University Research Foundation, 1941.
41. Livengood, J. C. and Wu, P C., "Correlation of autoignition phenomena in internal combustion engines and rapid compression machines," Symposium (international) on combustion 5:347-356, 1955.

Contact Information

Corresponding author:

John E. Dec
Sandia National Laboratories
MS 9053, PO Box 969
Livermore, CA 94551-0968, USA

Acknowledgments

The authors would like to thank Tim Gilbertson, Keith Penney, Gary Hubbard, and Alberto Garcia for their dedicated support of the LTGC Engine Laboratory.

This work was performed at the Combustion Research Facility, Sandia National Laboratories, Livermore, CA, Support was provided by the U.S. Department of Energy, Office of Vehicle Technologies. Sandia National Laboratories is a multi-mission laboratory managed and operated by National Technology and Engineering Solutions of Sandia, LLC., a wholly owned subsidiary of Honeywell International, Inc., for the U.S. Department of Energy's National Nuclear Security Administration under contract DE-NA0003525.

Definitions/Abbreviations

A_i	Pre-exponential factor of the specific reaction rate of reaction *i*
AKI	Anti-Knock Index = (RON + MON)/2
BDC	bottom dead center
BMON	blending motor octane number
BRON	blending research octane number
CAD	crank angle degrees
CA10	crank angle of 10% burn point
CA50	crank angle of 50% burn point
CI	compression ignition
C_p	heat capacity at constant pressure
DI	direct injection
E10	10% ethanol
E_a	activation energy
EGR	exhaust gas recirculation
E.P.A.	U.S. Environmental Protection Agency
F/A_{st}	fuel-air mass ratio at stoichiometric conditions
F/C	mass ratio between fuel and air + EGR
FACE	fuel for advance combustion engines
GDI	gasoline direct injector
HC	hydrocarbon
HCCI	homogeneous charge compression ignition – a well premixed form of LTGC
HOV	heat of vaporization
HRR	heat release rate
HTHR	high-temperature heat release
IMEP	indicated mean effective pressure
ITHR	intermediate-temperature heat release
LLNL	Lawrence Livermore National Laboratory
LTC	low temperature combustion
LTGC	low temperature gasoline combustion
LTHR	low temperature heat release
LVF	liquid volume fraction
MON	motor octane number
NO_x	oxides of nitrogen
NTC	negative temperature coefficient
NVO	negative valve overlap
P_{in}	intake pressure
PRF	primary reference fuel
RD5-87	research-quality, regular-grade E10 gasoline
RON	research octane number
S_i	sensitivity coefficient of reaction *i*
SI	spark ignition
T_{BDC}	temperature at bottom dead center
TDC	top dead center
X_{O2}	molar fraction of oxygen
φ	equivalence ratio
φ_m	equivalence ratio based on the total charge mass
τ	ignition delay

Appendix A: Single-component fuels taken into account to design tailored fuel blends

Table A1 shows the 16 different single-component fuels that are taken into account to design tailored fuel blends that maximize the φ-sensitivity. As it can be seen in the Table, they are classified as high-reactivity fuels (CA50 ≤ 368.5 CAD) or low-reactivity fuels (CA50 > 368.5 CAD) depending on the CA50 shown in an IC-reactor under base conditions (P_{in} = 2.5 bar, T_{BDC} = 360 K, φ_m = 0.40, X_{O2} = 12.6%).

Table 1A. Single-component fuels tested in this investigation.

Hydrocarbon class	Species	CHEMKIN formula	Reactivity
Paraffins	N-pentane	NC5H12	High
	N-heptane	NC7H16	High
Iso-paraffins	Iso-pentane	IC5H12	High
	Iso-heptane	C7H16-2	High
	Iso-octane	IC8	Low
Cyclo-paraffins	Cyclo-pentane	CPT	Low
Aromatics	Toluene	C6H5CH3	Low
	P-xylene	P-XYL	Low
	1,2,4 tri-methyl-benzene	T124MBZ	Low
Olefins	2-pentene	C5H10-2	Low
	1-hexene	C6H12-1	High
	Di-iso-butylene	IC8D4	Low
Oxygenated	Ethanol	C2H5OH	Low
	Iso-propanol	IC3H7OH	Low
	Iso-butanol	IC4H9OH	Low
	Iso-pentanol	IC5H11OH	High

Appendix B: Threshold that defines useful working conditions for LTGC engines

A threshold that defines the useful operating conditions for LTGC engines is obtained in this Appendix. To do so, the Livengood & Wu integral [41] is applied to the IC-engine simulation with RD5-87 at P_{in} = 1.0 bar (the least reactive condition tested in this investigation).

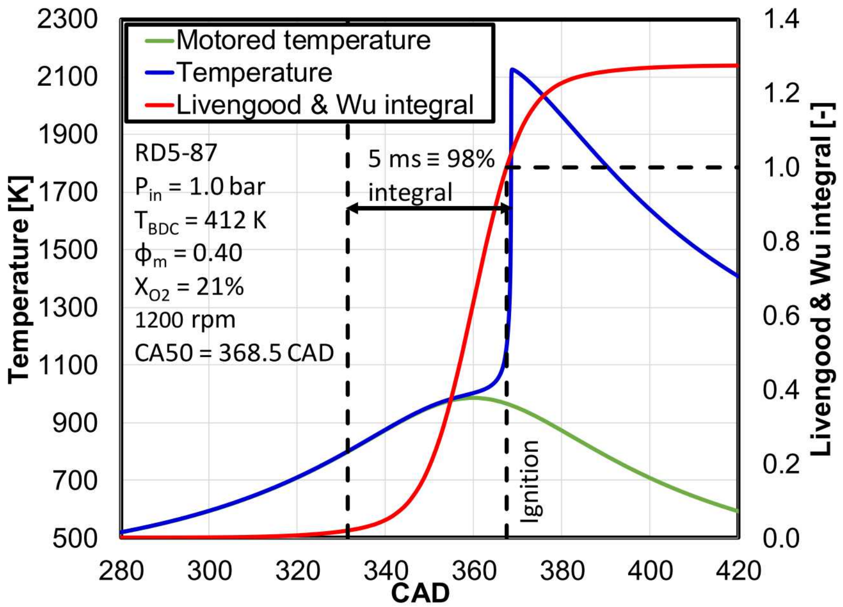

Figure B1. Temperature evolution with and without combustion for RD5-87 at naturally aspirated conditions. The Livengood & Wu integral has been applied to estimate the CAD range that effectively contributes to the ignition.

Figure B1 shows the temperature evolution with and without combustion for RD5-87 under naturally aspirated conditions. The BDC temperature (initial temperature in the simulations) is adjusted to obtain a CA50 = 368.5 CAD. The in-cylinder thermodynamic conditions that result from a simulation with the chemistry turned off are imposed in a 0-D, adiabatic, closed, constant-volume reactor to obtain the ignition delay that corresponds to each pressure – temperature combination. These ignition delays are used to compute the Livengood & Wu integral, which is plotted in red in the figure. Under these conditions, 98% of the integral is accumulated in the last 5 ms before the ignition. This means that conditions at which $\tau > 5$ ms are not useful for LTGC engines, since the ignition timescale is too long.